Summer 8-15-2019

Mesothelium-derived factors shape tissue resident macrophage

Chin-Wen Lai
Washington University in St. Louis

WASHINGTON UNIVERSITY IN ST. LOUIS

Division of Biology & Biomedical Sciences
Immunology

Dissertation Examination Committee:
Thaddeus S. Stappenbeck, Chair
Paul M. Allen
Michael S. Diamond
Brian T. Edelson
Emil Unanue
Wayne Yokoyama

Mesothelium-Derived Factors Shape Tissue Resident Macrophage

by
Chin-Wen Lai

A dissertation presented to
The Graduate School
of Washington University in
partial fulfillment of the
requirements for the degree
of Doctor of Philosophy

August 2019
St. Louis, Missouri

Table of Contents

List of Figures

CHAPTER 2

CHAPTER 3

List of Abbreviations

3D	Three dimensional
α-SMA	α-smooth muscle actin
ANOVA	Analysis of variance
APC	Adenomatous polyposis coli
Gata6	GATA Binding Protein 6
IBD	Inflammatory bowel disease
i.v.	Intravenous
i.p.	Intraperitoneal
KO	Knockout
LCM	Large cavity macrophage
MPF	Megakaryocyte potentiating factor
Msln	Mesothelin
Muc16	Mucin 16
PBS	Phosphate buffered saline
PFA	Paraformaldehyde
Poly(I:C)	Polyinosinic-polycytidylic acid
qRT-PCR	Quantitative real time polymerase chain reaction
RA	Retinoic acid
SEM	Standard error of the mean
TRM	Tissue resident macrophage
WAE	Wound associated epithelium
WT	Wild-type

Acknowledgements

First of all, I would like to thank Thaddeus Stappenbeck for being an exemplary mentor. His enthusiasm for science is contagious, and I have learned a great deal about experimental design, analytical thinking, and clear scientific writing under his guidance. Even though my thesis project ended up to be something unrelated to what he is really interested in, I appreciate all the support and encouragement he has given me these past years.

I would also like to acknowledge the members of my thesis committee. Their broad thinking and rigorous questioning has strongly shaped my project, and I appreciate all of their input during and outside of committee meetings. We came up the idea that not hanging around the non-interpretable result but moving forward toward something publishable. I am grateful that they have taken so much time to invest in my project an in my development as a scientist.

I thank the past and present members of the Stappenbeck lab. I have also had a lot of fun in this lab and everywhere I can find these people! It has been a great learning and social environment, and I have made lifelong friends here.

Many thanks to the administrative staff of Melanie Relich, Ann Winn, and everyone for making my thesis pan out, keeping me on track, answering questions, and providing lots of free food throughout the years. Thank you also to Gwendalyn Randolph, who has been and continues to be an excellent director of the Immunology program after Paul Allen and Gene Oltz.

I am also grateful for the love and support of my friends. The DBBS class of 2013 has been a wellspring of support (and valuable expertise and reagents), especially my peers: Prachi Bagadia, Nicholas Jarjour, and Rachel Wong. It has been wonderful to work on getting PhD at the same time with these talented and intelligent people.

I would also like to thank my friends outside of the program, who remind me that there is a world outside of the lab, especially my Taiwanese clubs and volleyball/softball teams. They provide me the place to relax and jump out of the box to think differently. It has been a wonderful journey to embrace multicultural perspectives and broaden my point of view from Taiwan.

Of course, I would to thank my family. I would not be where I am today if not for my parents and everything they have done for me. My brother is wonderful, and I know I can always count on him. I would also like to thank my wife who hasn't showed up but look forward to seeing you soon.

Funding for this work has been provided by Lucille P. Markey Special Emphasis Pathway in Human Pathobiology and the Crohn's & Colitis Foundation and the Rainin Foundation.

Chin-Wen Lai

Washington University in St. Louis

Aug 2019

ABSTRACT OF THE DISSERTATION

Mesothelium-derived factors shape tissue resident macrophages

by

Chin-Wen Lai

Doctor of Philosophy in Biology and Biomedical Sciences

Immunology

Washington University in St. Louis, 2019

Professor Thaddeus S. Stappenbeck

The studies outlined in this thesis provide several new insights into Msln-related pathways necessary for peritoneal immune responses and mucosal repair. We found that Msln and its binding partner mucin 16 from mesothelium influenced peritoneal and pleural macrophage differentiation. We found that Msln was required for proper tissue repair after colonic biopsy injury and was required for maximal polyp growth in $APC^{Min/+}$ mice. Overall, this work describes mesothelial and epithelial-derived factors that are important for tissue resident macrophage differentiation and wound repair after colonic mucosal injury. Understanding the complex interactions between stromal cells and immune cells will lead to better treatments for intestinal diseases such as inflammatory bowel disease and tumor associated macrophage-mediated tumorigenesis.

CHAPTER ONE: INTRODUCTION

Development of Tissue Resident Macrophage

Chapter 1: Introduction

Tissue resident macrophages

Macrophages were first described by Élie Metchnikoff in 1883[1]. They are widely distributed throughout the body and are present in the lymphoid organs, liver, lungs, gastrointestinal tract, central nervous system, bone, and skin. Macrophages are critical components of the innate and adaptive immune responses, and they are the first line of defense against foreign invaders through phagocytosis of pathogens[2,3]. The recent outburst of interest in genetic, evolutionary, and biochemical aspects of host-pathogen interactions has rekindled scientific interest regarding macrophages. Macrophages display great phenotypic and functional diversity due to their adaptation to their microenvironment. At the beginning of macrophage studies, researchers used bone marrow-derived macrophages (BMDM), which are primary macrophages derived from bone marrow (BM) cells *in vitro* in the presence of growth factors Macrophage colony-stimulating factor (M-CSF)[4]. BM yielded the most macrophages with the best homogeneity but it does not represent adequate *in vivo* primary responses. In the past decade, new insights have been expanded in the origin of tissue-resident macrophages. First, these cells are derived from three progenitors, including yolk sac macrophages, fetal liver monocytes and circulating monocytes[5,6], which replenish the niches consistently since embryogenesis. Second, even residing in distinct microenvironments, tissue-resident macrophages have several common features: the ability to phagocytize pathogens and dying cells, the production of cytokines and chemokines to initiate immune responses, and the expression of markers such as CD11b, F4/80 and CD64 on the cell surface of murine tissue-resident macrophages[7-10].

Next to these common features, each tissue resident macrophage population has a unique identity and function. Interestingly, this functional specialization is dependent on the tissue in which they reside. For example, tissue resident macrophages located in the brain, called microglia, are small star-shaped cells and involved in brain surveillance by constantly sensing the cellular environment. They play important roles in brain development and homeostasis by regulating the synaptic carving during postnatal development[11]. Another example is the lung alveolar macrophages which are responsible for the clearance of alveolar surfactant[12]. The tissue-specific function of these macrophages implies that they must have a different functional identity. Furthermore, tissue-specific signals which regulate the expression or activity of signal-dependent transcription factors (TFs) govern this functional specialization and adapt the core macrophage program by activating functional modules, which gives macrophages their functional identity. Niche signals from unique microenvironment also guide the differentiation and development of tissue resident macrophages.

Transcription factors and niche signals involved in tissue-resident macrophage development

Macrophages form a diverse group of mononuclear phagocytes. Regardless of this heterogeneity, all macrophage populations share a large transcriptional network and epigenetic landscape. This core macrophage program is established by a group of lineage-determining TFs which perform a general role in myelo-monocytic development by determining stem cell fate.

PU.1 is one of the most well studied principal regulators in macrophage development[13]. PU.1 determines myeloid progenitor fate in a concentration-dependent manner in the process of the early stages of myeloid cell development. A high level of PU.1 leads to the macrophage development whereas a low amount of PU.1 is necessary for B cell development[14]. In the detailed regulation,

this concentration-dependent effect can result from the numerous low- and high-affinity PU.1 binding sites present in the genome[15]. The low-affinity binding sites are only bound by PU.1 when it reaches a certain threshold concentration. One of the major target genes of PU.1 in macrophage development is *Csf1r*, which encodes the receptor for M-CSF (M-CSFR/CD115) and interleukin-34 (IL-34). M-CSF is critical in survival, maintenance and proliferation of most mononuclear phagocytes, whereas IL-34 is specifically required for the development and maintenance of Langerhans cells and microglia[16,17]. Together, PU.1 and Csf1r are essential for the formation of yolk sac macrophages[18]. Generally, PU.1 regulates tissue-resident macrophage development by acting as a scaffold for histone modifiers. In addition, many TFs involved in tissue-resident macrophage development, function and activation perform their function through interaction with PU.1. For instance, it was shown that c-Jun can enhance the ability of PU.1 to drive expression of M-CSFR[19].

Upon terminal differentiation, MafB expression drives tissue-resident macrophages to exit the cell cycle[20]. MafB, synchronizing with c-Maf, desensitize macrophages from the M-CSF-mediated proliferative effect by blocking the expression of self-renewal genes such as *Myc, Klf2* and *Klf4*[21]. This acts through direct inhibition of macrophage enhancers, including PU.1. In self-maintaining tissue-resident macrophage populations, differentiated tissue-resident macrophages can re-enter the cell cycle by temporarily pausing the inhibition of these enhancers. Contrary to regenerative processes, dedifferentiation of the tissue-resident macrophages does not happen[22]. In addition, MafB plays a key role in F4/80 maturation[23] and involves in actin remodeling[24].

Other lineage-determining TFs have been mentioned, including Batf3, Pparg, Irf8[25]. However, it is not clear whether these factors are essentially required for macrophage development. Moreover, it is unknown whether macrophages require continuous expression of these factors for their function, maintenance, or survival. Together, these lineage-determining TFs establish the core macrophage program, including Cx3cr1, phagocytic receptors, Fcγ receptors (e.g. Fcgr1, encoding CD64), pattern recognition receptors, Mertk and Adgre1 (F4/80) in the pre-macrophage commitment by almost all macrophage populations[8,25-27]. Additionally, these lineage-determining TFs can shape the epigenome and form an anchor point for signal-dependent TFs accordingly.

Although sharing many similarities, identity and function among all the macrophages are very diverse and unique for each tissue, implicating that the core macrophage program has to be adapted in a tissue-dependent manner. According to the niche hypothesis[28], the particular niche provides physical support and nurtures the local tissue resident macrophages through the production of niche signals. By driving signal-dependent TF expression or activation, cytokines, metabolites, and cell-cell contacts may all be the niche signals which initiate tissue-specific transcriptional networks in the pre-macrophages upon emigration[29]. These local signal-mediated TFs orchestrate with lineage-determining TFs to fine-tune the core macrophage program and imprint a unique transcriptional program in the tissue-resident macrophage. This is done through direct activation of signature genes or by inducing chromatin remodeling which enables signal-dependent TFs to active signature genes. These signature genes are often necessary for the functional maturation and/or survival of tissue-resident macrophages to meet the tissue-specific prerequisites.

Peritoneal macrophage

As a cellular source, scientists have performed studies using peritoneal macrophages and we have gained a representative portion of the current knowledge regarding macrophage biology, such as their function, specialization, and development. However, it was described recently the existence of two resident macrophage subsets present in the peritoneal cavity. According to their size, these macrophage subsets were labeled LPM and SPM[30]. In addition to the size, they were designated by their differential expression of F4/80 and CD11b, where SPMs show F4/80^{low}CD11b^{low} phenotype while LPMs express high levels of F4/80 and CD11b. F4/80, a 160 kD glycoprotein from the epidermal growth factor-transmembrane 7 (TM7) family, is expressed by macrophages in most organs, and it is not detected on lymphocytes, polymorphonuclear cells, and fibroblasts[31]. To be noted, peritoneal eosinophils show low levels of F4/80[30] and some macrophage subpopulations exhibit low levels or do not express F4/80, such as white pulp and marginal zone splenic macrophages[32]. CD11b is an integrin that, together with CD18, forms the CR3 heterodimer[33], but is not exclusively expressed on macrophages and is found on several others cell types, including polymorphonuclear cells[34], DCs[35], and at low levels on B lymphocytes[36,37]. The other marker for LPM is ICAM2, a member of the intercellular adhesion molecule (ICAM) family, while SPMs express low ICAM2[27]. All ICAM proteins are type I transmembrane glycoproteins, contain 2-9 immunoglobulin-like C2-type domains, and bind to the leukocyte adhesion LFA-1 protein[38,39]. It mediates adhesive interactions important for antigen-specific immune response, NK-cell mediated clearance, lymphocyte recirculation, and other cellular interactions important for immune response and surveillance. It showed that retinoic acid regulates ICAM2 expression in LPMs[40]. SPMs phagocytose bacteria and make large amounts of nitric oxide[30]. Compared to SPMs, LPMs make much less nitric oxide and have less capacity to phagocytose bacteria. However, LPMs phagocytose apoptotic cells more effectively[41].

At steady state, LPMs appear to be maintained by self-renewal and independent of hematopoiesis[42,43], whereas SPMs are originated from circulating monocytes. Dates from Schulz et al. suggest that, in general, F4/80 expression by tissue macrophages correlated with yolk sac ($F4/80^{high}$) and not hematopoietic ($F4/80^{low}$) progenitors[44]. By using CX3CR1CreRosa26R-FGFP mice which mark the active and past expression of CX3CR1, the presence of GFP+ cells was found within DC, SPM, and LPM populations. Conversely, the presence of GFP^+ cells was in DC and SPM pool, but not in the LPM population in the $CX3CR1^{GFP/WT}$ mice. These data indicate that SPMs are short-lived cells, whereas LPMs have a more dynamic ontogenic relationship with a $CX3CR1^+$ progenitor. Meanwhile, in chimeric C57BL/6-CD45.2 mice reconstituted with C57BL/6-CD45.1 BM, the majority of LPMs and SPMs are CD45.1-derived cells, demonstrating that both macrophage subsets differentiate from BM precursors after irradiation-induced macrophage ablation[43]. The other group suggests that $Ly6C^+$ monocytes recruited during inflammatory conditions could give rise to SPMs[30] in a CCR2-dependent manner[45].

Data with mice lacking CCAAT/enhancer binding protein (C/EBP)beta also support the idea that LPMs and SPMs represent distinct ontogenies, because without this transcription factor, there are no LPMs and increased numbers of SPMs in the peritoneal cavity[43]. Interestingly, adoptively transferred SPMs differentiated into LPMs in *Cebpb*$^{-/-}$ mice. However, in control mice that have normal numbers of LPMs, only a small frequency of transferred SPMs acquired the $F4/80^{hi}MHCII^{low}$ phenotype of LPMs. These results indicated that SPMs appear to contribute in only a small way to generate LPMs at homeostasis, but SPMs could maintain the pool of LPMs in severe situations such as under inflammatory conditions or following radiation ablation[43]. The

findings of Yona et al.[42] also demonstrated monocyte-derived LPMs presented 8 weeks after thioglycollate injection. Together with LPMs, a subset of proliferating BM-derived inflammatory macrophage has also been associated with self-renewal mechanisms during the resolution of peritonitis induced by zymosan and thioglycollate[46]. Conversely, LPMs do not seem to contribute to the SPM pool, even during inflammation.

Intestinal macrophage

Macrophages play a variety of roles to maintain intestinal homeostasis. Like their counterparts in other tissues, intestinal macrophages are avidly phagocytic. However, intestinal macrophages-mediated phagocytosis in both mouse and man does not cause an overt inflammatory response[47-51]. Consistent with this role, intestinal macrophages display high expression of genes associated with phagocytosis, such as *Mertk, Cd206, Gas6, Axl, Cd36, Itgav*, and *Itgb5*[52,53]. Integrins αv and β5 dimerize to form αvβ5, which is involved in efferocytosis[54]. Notably, Lys2 deletion of integrin αv in myeloid cells results in the accumulation of apoptotic cells in the intestine[55], and Itgb5 deficiency predisposes to increased susceptibility to DSS-induced colitis, highlighting a particularly important role for this pathway in efferocytosis. The sub-epithelial positioning of lamina propria (LP) macrophages locates them to control bacteria invasion through epithelial barrier. In addition, murine studies have shown that they are able to sample luminal bacteria by transepithelial dendrites, cellular processes that cross the epithelial barrier without perturbing tight junctions and epithelial integrity and depend on the CX3CL1-CX3CR1 axis[56,57].

Though a peripheral monocyte to macrophage differentiation continuum exists in the intestinal LP, a process which is known as the monocyte "waterfall"[9,48], almost all other tissues contain locally

maintained macrophage populations that coexist with monocyte-replenished cells at homeostasis. It was not until recently that Tim-4^{+}CD4^{+} gut macrophages were found to be locally maintained[58], while Tim-4^{-}CD4^{+} macrophages had a slow turnover from blood monocytes. TGFβR signaling is essential for the terminal differentiation of intestinal macrophages. In particular, upregulation of genes associated with the homeostatic profile of intestinal macrophages, such as *Cx3crl*, *Itgb5,* and *Il10* relies on the TGFβ-TGFβR axis[52]. TGFβ-expressed intestinal macrophages in mucosa themselves may be important because efferocytosis is known to induce TGFβ expression in macrophages[59] and, at least in man, macrophages may activate TGFβ signaling pathway through integrin β8[60]. The high expression of CX3CR1 by murine intestinal macrophages and their positioning adjacent to CX3CL1-producing epithelial cells also imply the possibility of CX3CL1-CX3CR1-mediated macrophage differentiation[56,57].

In both ulcerative colitis (UC) and Crohn's disease (CD), accumulation of CD14^{hi}CD11c^{hi} monocytes/immature macrophages that come to outnumber CD64^{+}HLA^{-}DR^{hi}CD14^{lo} resident macrophages[48,50,61-63] is one of the features. In contrast to their homeostatic counterparts, these CD14^{hi} cells in the gut produce pro-inflammatory cytokines and chemokines, such as TNFα, IL1β, IL6, IL12, and CCL11[62,63], display respiratory burst activity[64] and respond to commensal bacteria abnormally. In addition, they express high levels of TREM1, which can potently amplify pro-inflammatory responses[65]. Importantly, mucosal healing in IBD patients receiving anti-TNF has been shown decreased CD14^{hi} cells and increased pro-reparative CD206^{+} macrophages[66].

Gata6

The GATA zinc finger transcription factors regulate the development and differentiation of several tissues. Through a conserved Cys-X2-Cys-X17-Cys-X2-Cys zinc finger protein motif, these factors bind the basic consensus sequence A/TGATA/G. Three members of the family, GATA1, GATA2 and GATA3, are all expressed in the haematopoietic system and a number of other tissues. Each appears to have a different function in the haematopoietic system. The other members of family, GATA4, GATA5 and GATA6, also show a partially overlapping expression pattern in the heart and the intestinal tract[67,68]. Murine GATA6 has been reported to be restricted to precardiac mesoderm, the embryonic heart tube and the primitive gut. It is also expressed in the developing respiratory and urogenital tracts, arterial smooth muscle cells, the bronchi, the urogenital tract and the bladder. Overexpression of GATA6 in the cardiac cells at a time when its expression normally declines (i.e. before the appearance of terminally differentiated markers) results in arrest of cardiomyogenic differentiation, indicating that the GATA6 gene may act in Xenopus to maintain the precursor status[69]. Thus the available data indicates that GATA6 may be important for heart development. The transcriptional factor Gata6 is specifically expressed by self-renewing peritoneal macrophages but not by monocytes recently recruited into the peritoneum after challenge. Gata6 deficiency impairs peritoneal macrophage renewal during steady state and in response to inflammatory challenge compromising the resolution of inflammation. Gata6 targets genes involved in cell proliferation since their expression is altered in macrophages from Gata6-deficient mice.

Mesothelium

The structure of mesothelium is a single layer of thin plate-like cells. The squamous mesothelia are polarized with their apical microvilli and cilia-rich surfaces toward the coelomic space[70,71].

Tight junctions located on the lateral aspect of the cell maintain apical/basal polarity and create a diffusion barrier between the coelomic space and the submesothelial connective tissue of the organ or body wall. Cytokeratins (mostly subtypes 8, 18, and 19) provide structural support and E-cadherin confers further cell-cell adhesion[72,73]. A basement membrane is produced by and underlies the mesothelium separating it from the sub-mesothelial connective tissue space. In mammals, separation of the common embryonic coelom gives rise to pericardial, pleural and peritoneal cavities. To further subdive, mesothelial cells lining the organs are referred to as visceral mesothelia while parietal mesothelia cover the organs cavities/body walls. Visceral mesothelium covering the heart is referred to as the epicardium while pleural mesothelium covers lungs. Serosal mesothelium covers the organs of the alimentary canal within the abdominal cavity/coelom. Despite the multiple names, mesothelium has a relatively consistent structure in each of the coelomic cavities.

The most conspicuous function of mesothelia in the adult is to produce a non-adhesive surface which allows frictionless movement of the organs within the coelomic cavity. The secretion of an apical glycosaminoglycan layer and production of a small amount of circulating coelomic fluid to provide lubrication are the key for this dynamic movement[74,75]. Submesothelial lymphatic vessels connect with gaps in the mesothelial monolayer called stomata on the surface of the diaphragm[70]. Mesothelium not only regulates ionic and protein composition of coelomic cavity fluid but also the passage of inflammatory cells[76,77]. Additionally, mesothelium is crucial to the injury response and is thought to both prevent and promote scarring depending on the injury and to promote neovascularization[78-80]. These and many other studies have provided growing evidence for the dynamic role of mesothelium in both normal and abnormal physiologic states in the adult[81].

Msln and Mucin 16

Msln is a glycophosphatidylinositol (GPI) –linked cell-surface glycoprotein. It is synthesized as a 71-kD precursor protein and is then cleaved by the endoprotease furin to release the secreted N-terminal region, called megakaryocyte potentiating factor (MPF), whereas the 41-kD mature Msln remains attached to the membrane[82,83]. The remaining GPI-linked mature Msln can also be shed from the cell through the action of the tumor necrosis factor α–converting enzyme protease[84]. The normal physiologic distribution of Msln identifies it as a differentiation factor for mesothelial cells, but the biologic role that Msln plays in these cells remains unclear. Database searches reveal that Msln is remotely homologous to two inner ear proteins of unknown structure and contains no conserved consensus domains[85]. Three-dimensional structure prediction programs have determined that Msln consists of a superhelical structure with armadillo-type repeats[86]. No crystal structure has yet been determined for the whole protein, but the structure of an N-terminal fragment bound to a Fab of the SS1 antibody has been obtained[87]. Furthermore, Msln knockout mice grow and reproduce normally and have no detectable phenotype[88].

Msln is expressed by many solid tumors, with particularly robust expression in mesothelioma, epithelial ovarian cancer, and pancreatic adenocarcinoma[89-92]. Higher expression of Msln has been correlated with poorer prognosis for patients with ovarian cancer[93], cholangiocarcinoma[94], lung adenocarcinoma[95], triple-negative breast cancer[96], and resectable pancreatic adenocarcinoma[97]. In the neoplastic setting, Msln is known to bind to the ovarian cancer antigen Muc16 (cancer antigen 125)[98]. Muc16 is a membrane spanning mucin that is expressed on ovarian, endometrial, tracheal, and ocular surface epithelial cells. This mucin is initially expressed on the surface and then shed in the extracellular milieu following proteolytic cleavage. The two proteins are frequently

coexpressed, and binding of Msln and Muc16 has been shown to induce cell-to-cell adhesion in these cell types[99]. Muc16 expressed on cancer cells can also facilitate cancer cell attachment to the Msln-expressing serosal surfaces in the pleura and peritoneum, possibly contributing to peritoneal seeding and metastatic spread. In addition, signaling mediated by Msln and Muc16 binding has been reported to increase cellular resistance to anoikis[100], upregulate matrix metalloproteinases important in cellular invasion and metastasis[101], and induce secretion of autocrine growth factors by constitutively activating nuclear factor kappa B (NF-κB)[102,103]. However, it seems that Msln expression may also trigger signaling events independent of Muc16 binding[90]. The exact mechanics of these pathways and how Msln interacts with components of the tumor micro-environment, including stromal cells, the extracellular matrix, and immune-cell populations, are not known.

Why Msln, a glycoprotein normally restricted to serosal cells of the pleura, peritoneum, and pericardium, is expressed in a wide variety of adenocarcinomas is not clear at this time. However, regulation of Msln expression in tumors has been assessed in several studies and seems to be cell-type specific. At the epigenetic level, it was found that hypomethylation did not correlate with Msln expression in ovarian or endometrial cancer specimens or in mesothelioma[104]. However, hypomethylation of the promoter was noted in Msln-expressing pancreatic cancer specimens, and treatment of a nonexpressing pancreatic cancer cell line with demethylating agents could induce expression of Msln, suggesting that epigenetic mechanisms may regulate Msln expression in this cell type[89]. Transcription of Msln is driven by a TATA-less promoter located upstream of the transcriptional start site. Enhancers responsible for initiating strong expression in normal serosal cells and cancers derived from them (eg, mesothelioma and ovarian cancer) are unknown. Cancer-

specific ectopic upregulation in pancreatic and cervical cancers has been attributed to the transcriptional enhancer factor 1 (TEF-1) transcription factor binding to a conventional MCAT sequence within an upstream enhancer region called CanScript. However, TEF-1 expression itself is necessary but not sufficient to induce Msln expression, suggesting an unknown cofactor is also required[105]. Similarly, the yes-associated protein 1 (YAP1) transcription factor binds to an SP-1 motif within the CanScript and is also required but insufficient for MSLN expression[106]. Further study will be required to delineate this mechanism. More recently, it was discovered that Msln is reciprocally regulated at the post-transcriptional level by mIR-198 as part of a feedback loop that involves NF-kB and the homeobox transcription factors octamer transcription factor 2 (OCT-2), pre–B cell leukemia homeobox 1 (PBX-1), and valosin-containing protein[107].

Recently more researches delineate the role of Msln in non-tumorigenesis condition. One group determined that Msln facilitates both TGF-β1–induced activation of activated portal fibroblasts (aPFs) and FGF-induced proliferation of aPFs[108]. And the mice lacking Muc16 had similar results in the murine liver fibrosis model. They also detected a similar upregulation of Msln+ aPFs in patients with biliary fibrosis of different etiologies. The other group found up-regulation of Msln in both human and murine peritoneal adhesions, which indicated that Msln expression correlated to injury-induced inflammation[109]. Upon injury, many activated fibroblasts share similar mesothelial markers. And one of the studies demonstrate that human Muc16 inhibits the cytolytic functions of both human and murine NK cells and macrophages to a similar degree. These studies are important steps in using mouse models to delineate the immuno-regulatory roles of Msln/Muc16 that provide immune protection to ovarian and other epithelial tumors. Several recent studies highlight the need to investigate the effects of Muc16 on immune cells[110]. Most importantly,

the correlation of decreased therapeutic responses of farletuzumab and amatuximab in patients with higher circulating levels of Muc16 and the ability of this mucin to perturb interactions between therapeutic antibodies and Fc-γ receptors are raising the possibility that Msln/Muc16 and other mucins could influence the success of some anti-cancer immunotherapies[111].

Model of peritonitis

Infectious peritonitis triggered by the injection of pathogens into the peritoneal cavity has been used as a model to study innate immunity during acute inflammation since the time of Mechnikov. However, infectious peritonitis models are hard to control because the exact time course of the inflammatory response depends on both the pathogenicity and growth rate of the specific microorganisms used and the magnitude and efficacy of the host immune responses. Experimental animal models can be used to study specific aspects of the pathophysiology of peritonitis as it presents in the clinic, and these models provide platforms for illuminating the general mechanisms of inflammation and testing novel anti-inflammatory strategies. For instance, the cecal ligation and puncture (CLP) model mimics the polymicrobial sepsis[112].

The intraperitoneal injection of a wide range of irritants leads to an acute inflammatory response that peaks within hours, including thioglycollate broth[113] and inflammatory cytokines[114]. Injection of zymosan, the insoluble polysaccharide cell wall component derived from *Saccharomyces cerevisiae*, is a popular self-resolving model of peritoneal inflammation in mice, which induced all the hallmarks of acute inflammation, including pain, leukocyte infiltration, and synthesis of inflammatory mediators including leukotrienes and prostaglandins[115]. It provides a direct analog of many of the features observed in *in vitro* zymosan-treated macrophages. Macrophage

recognition of unopsonized zymosan *in vitro* is β-glucan receptor dectin-1 dependent[116]; whereas collaborative signaling from TLR2 by an MyD88-dependent signaling pathway induces the generation of inflammatory mediators. *In vivo* Peritonitis experiments also show dectin-1 recognized zymosan and controlled fungal infection[117].

Zymosan-induced peritonitis model has several advantages over other reagents. First, the mild-to-moderate severity of the injury (which can be varied with the dose of zymosan) means that inflammation self-resolves within 48 to 72 h, mimicking the normal inflammatory response of an immunocompetent individual. Second, the model allows collection of a reasonable amount of exudate for analyzing multiple inflammatory mediators. Third, injection into a serosal cavity means that leukocytes exit from the site of inflammation by way of their natural conduits to the draining lymph node[118,119]. Finally, this model enables a wide range of researches due to the relative technical simplicity and reproducibility. In addition, because peak neutrophil levels occur within 3-4 h of a $2x10^6$ zymosan particles injection, it is convenient to generate and analyze data within a short time frame.

Models of colonic injury

The tube-shaped colon is composed of several layers. The inner-most layer is the epithelial layer, which separates the contents of the lumen from the host. The mesenchymal layer which includes neuronal, stromal, and hematopoietic cells is adjacent and supporting the epithelial layer. Together, these two layers are called the mucosa. The next radial layer is the submucosa composed of muscularis propria, including the circular and longitudinal muscle layers. The outer-most radial layer of the colon is the single-mesothelial-cell serosal layer.

The colonic epithelium is composed of many invaginations called crypts of Lieberkuhn. The highly proliferative epithelial stem cells reside at the base of the each crypt and divide to produce progenitors and more stem cells. The progenitors divide and differentiate into absorptive enterocytes, secretory goblet cells, or enteroendocrine cells. The mature epithelial cells move up from the crypt to reach the top and undergo apoptosis. Their migration away from canonical Wnt signaling that enriches at the base of the crypts drives the differentiation of progenitors and benefits the maintenance of homeostasis; however, during inflammation or infection, the compromised barrier function drives mucosal repair through the overwhelming epithelial renewal. Various injury models in mice have been used to study the mechanisms for colonic immune-epithelial interaction after injury and to gain novel treatments to stimulate intestinal repair.

Many animal models of inflammatory bowel disease (IBD) recapitulate certain aspects of the human disease[120]. For instance, administration of chemicals like dextran sodium sulfate (DSS)[121] or 2,4,6-trinitrobenzene sulfonic acid (TNBS)[122] leads to significant epithelial damage and inflammation. Other models of IBD include cell transfer models (adoptive transfer of $CD4^{+}CD45RB^{high}$ T cells)[123] and genetic models (e.g. IL-2 or IL-10 KO mice). There are other models of intestinal epithelial damage such as radiation, ischemia/reperfusion, and Clostridium difficile infection that all lead to intestinal inflammation and/or loss of crypts. Given IBD results from abnormal crosstalk between genetics and the environment, these models help identifying important mediators of inflammation such as cytokines and bacterial products.

Our lab has used the murine colonic biopsy injury system to study mechanisms of epithelial repair[124]. To create mucosal wounds, we insert a pair of forceps into the colon of an anesthetized mouse and remove around 300 crypts and the mesenchymal layer but not cause perforation. This system is ideal for studying the mechanisms of temporal and spatial mucosal repair. This system can be used to study mice that are genetically deficient for genes that are known to be important in mucosal repair and discover novel genes important in mucosal repair.

CHAPTER TWO

Mesothelial niche Msln and mucin 16 shape tissue resident macrophage differentiation

Chapter 2: Abstract

The local cellular environment of each tissue is thought to play a role in shaping resident macrophage differentiation state. In the peritoneal cavity, dietary retinoic acid has previously been shown to polarize macrophages in this location through the reversible induction of a transcription factor which defines LPM identity, Gata6. We hypothesized that local factors in the peritoneum could also support tissue-specific differentiation of macrophages. We found that soluble proteins from the peritoneum upregulated Gata6 expression in stimulated LPMs. We investigated mesothelial cells because of their known function in secreting factors into the peritoneal fluid and their interactions with resident immune cells. Analysis of their global gene expression highlighted Msln and its binding partner Muc16 as candidate ligands to regulate Gata6 expression in LPMs. We found that mice deficient for either of these molecules showed diminished Gata6 and F4/80 positive LPMs in homeostasis. Pleural cavity macrophages, similarly to LPMs, display lower Gata6 and F4/80 expression in *Msln*$^{-/-}$ and *Muc16*$^{-/-}$ mice, suggesting that Msln and Muc16 exhibit generalizable effects across cavities derived from the intraembryonic coelom. Compared to wild-type recipient mice, lethally irradiated *Msln*$^{-/-}$ and *Muc16*$^{-/-}$ mice reconstituted with wild-type bone marrow have lower Gata6 and F4/80 expression in LPMs and pleural cavity macrophages. Similarly, during the resolution of zymosan-induced inflammation, repopulated LPMs expressed diminished Gata6 and F4/80 in the absence of Msln or Muc16, suggesting these ligands have the extrinsic impact on resident macrophage differentiation. Overall, we found novel tissue-specific factors that regulate differentiation of resident macrophages in mesothelium lined cavities.

Chapter 2: Introduction

Macrophages are members of the mononuclear phagocytic system that reside in every organ[3,125,126]. These cells play important roles in a variety of important processes including the initial control of infection and response to tissue damage. To execute their functions in the context of specific organs, tissue resident macrophages (TRMs) must adapt to their local environment[27,127-130]. The specialization of TRMs occurs by the instruction of specific transcription factors that are induced by factors within the microenvironment[131]. TRM phenotypes can be defined by a combination of multiple transcription factors that control the functional programs of these cells.

In the peritoneal cavity, LPMs are the dominant TRMs that functionally mediate type 2 immunity, facilitate the tissue repair of the mesothelium, and protect against peritoneal fibrosis[30,132,133]. LPMs require the induction of transcription factors, including C/EBPβ[43] and Gata6[40,134,135]. Gata6 deficiency results in dysregulated peritoneal macrophage proliferative renewal during homeostasis and in response to inflammation, which is associated with delays in the resolution of inflammation[135].

Previous studies have shown that local factors play key roles in promoting the ontogeny and phenotype of TRMs[133,136]. Among factors known to be important for LPM function[40,134,135,137], omentum-derived retinoic acid (RA) induces Gata6 expression in LPMs[40,127] which in turn regulates gene expression of factors that define peritoneal macrophages. It is still unclear whether RA is the sole local factor that regulates Gata6 expression in LPMs.

Mesothelial cells are important tissue factor producers due to their immediate proximity to the serosal cavities. In addition to roles in the pleura and pericardium[70,138], mesothelial cells line the entire peritoneal cavity and produce a protective, non-adhesive barrier against physical and biochemical damage from infection and surgery[76,77]. Mesothelial cells play key roles in fluid transport and inflammation, as reflected in their expression of proteins such as solute transporters, adhesion molecules, cytokines, growth factors, and reactive oxygen species. These cells also express a wide range of lineage markers, including the adhesion protein mesothelin (Msln)[139] and its binding partner mucin 16 (Muc16)[140].

We hypothesize that mesothelial cells can communicate with LPMs to affect their differentiation state and function through modulation of Gata6 expression. We found that a high molecular-weight complex in the peritoneal fluid contains the secreted proteins, Msln and Muc16, which preserve Gata6 expression in isolated and cultured LPMs. We further identified that Msln and Muc16 play key roles during in the extrinsic control of Gata6 expression in LPMs and pleural macrophages during homeostasis and injury. Collectively, these data delineate a role for soluble, micro-environmental factors in regulating tissue macrophage identity.

Chapter 2: Methods and Materials

Methods

Mice

C57BL/6J (CD45.2) and B6.SJL (CD45.1) mice were obtained from Jackson Laboratories. *Msln*$^{-/-}$ [88] and *Muc16*$^{-/-}$ mice[141] on the C57BL/6 background were provided by Dr. Ira Pastan (National Cancer Institute, USA) and Dr. Robert C. Bast (MD Anderson Cancer Center, USA), respectively. Lyz2 Cre x *Gata6*$^{flox/flox}$ and *Gata6*$^{flox/flox}$ littermate controls were provided by Dr. Gwendalyn J.

Randolph and generated as previously described[134]. All mice were used for experiments were between 8 and 12 weeks of age unless otherwise stated and were maintained in one of two specific pathogen-free barrier facilities. Sex-matched littermates were used for experiments whenever possible, although in some cases mice from multiple litters were used in a single experiment. All animal experiments were approved by the Animal Studies Committee of Washington University in St. Louis.

Leukocyte Collection

Peritoneal and pleural cells were collected from body cavities by lavage with 0.5% BSA and 2 mM EDTA in 1x PBS (FACS buffer). Spleen and Peyer's patches were excised, placed in sterile FACS buffer, and finely minced. Cellular suspensions were passed through a 70 μm cell strainer before analysis. If lysis of red blood cells was necessary, cell suspensions were treated with Red Blood Cell Lysis Buffer (Sigma) according to the manufacturer's protocol. Live cells were counted with Countess II FL cell counter (Invitrogen) using a Trypan Blue stain for dead cell exclusion.

Flow Cytometry

Cells were stained for surface markers by blocking with α-CD16/32 (clone 2.4G2, Tonbo) for 10 minutes at 4 ºC followed by staining for 20 min at 4 ºC before running on a flow cytometer in FACS buffer. Cells which were to be stained intracellularly were first stained for surface markers and then were stained as indicated by the FoxP3/Transcription Factor Staining Buffer set (eBioscience). In brief, surface stained cells were fixed, permeabilized, and stained with either Gata6 or Ki67 for 20 min at 4 ºC, followed by washing once in 1x Perm/Wash buffer and then resuspension in FACS buffer before flow cytometric analysis.

Single-cell preparations were stained with antibodies to the following markers: anti-B220 (clone RA3-6B2; BioLegend), anti-CD3 (clone 17A2; BioLegend), anti-CD4 (clone RM4-5; BioLegend), anti-CD5 (clone 53-7.3; BioLegend), anti-CD8a (clone 53-6.7; BioLegend), anti-CD11b (clone M1/70; BioLegend), anti-CD11c (clone N418; BioLegend), anti-CD19 (clone 1D3; BioLegend), anti-CD45.1 (clone A20; BioLegend), anti-CD45.2 (clone A104; BioLegend), anti-CD102/ICAM2 (clone 3C4; BioLegend), anti-CD105 (clone MJ7/18; BioLegend), anti-CD115 (clone AFS98; BioLegend), anti-CD117 (clone 2B8; BD), anti-CD135 (clone A2F10.1; BD), anti-CD138 (clone 281-2; BioLegend), anti-F4/80 (clone BM8.1; eBioscience), anti-Gata6 (clone D61E4; Cell Signaling Technologies), anti-GL7 (clone GL7; BD), anti-MHC-II (clone M5/114.15.2; BioLegend), anti-Ki67 (clone SolA15; eBioscience), anti-Ly6C (clone HK1.4; BioLegend), anti-Ly6G (clone 1A8; BioLegend), anti-GPM6a (clone 321; MBL), anti-NK1.1 (clone PK136; Tonbo), anti-Pdpn (clone 8.1.1; BioLegend), anti-SiglecF (clone E50-2440; BD), anti-streptavidin (Thermo), anti-TER119 (clone TER-119; BioLegend), and anti-Tim4 (clone RMT4-54; BioLegend).

In experiments to assess cell death, cell suspensions were washed once in 1x PBS, resuspended in Annexin binding buffer, and stained with FITC-conjugated Annexin V and Propidium Iodide as per the manufacturer's instruction (BD). Flow cytometry was performed on FACS Canto II, LSR Fortessa, LSR Fortessa X20, or LSR II instruments (BD). FlowJo software (Treestar) was used for analysis.

All cells were first gated on a FSC/SSC gate and a FSC-W/FSC-A singlet gate. Peritoneal and pleural macrophages were gated as $CD115^+$ $CD11b^+$ and then divided into $ICAM2^+$ $MHC\text{-}II^{lo}$ large macrophages or ICAM2- MHC-II+ small macrophages. Peritoneal eosinophils were gated as $Siglec\text{-}F^+$ $CD11b^{int}$, and peritoneal B cells were gated as $CD115^-$ $CD19^+$ $MHC\text{-}II^+$. In the spleen and Peyer's patches, B cells were gated as $B220^+$ $CD3^-$, plasma cells as $B220^+$ $GL7^+$, and germinal center B cells as $B220^-$ $CD138^+$. $CD4^+$ T cells were gated as $CD3^+$ $CD4^+$, and $CD8^+$ T cells as $CD3^+$ $CD8^+$. NK cells were gated as $NK1.1^+$ $CD3^-$, and neutrophils were gated as $Ly6C^+$ $Ly6G^+$. Red pulp macrophages were gated as $F4/80^{hi}$ $CD11b^{lo}$ $MHC\text{-}II^{lo}$ $CD11c^{lo}$. Common monocyte precursor (cMoP) cells were gated as $cKit^{lo}$ $Flt3^-$ $CD115^+$ $Ly6c^{hi}$ $CD11b^+$ $CD11c^-$ $Ly6G^-$.

LPM and BM-Monocyte Sorting

Large peritoneal macrophages were sorted from peritoneal exudate cells using a $CD11b^+$ $ICAM2^+$ $F4/80^+$ gating strategy. Monocytes were isolated from red blood cell lysis buffer–treated bone marrow cell suspensions using immunomagnetic depletion of T cells, B cells, DCs, granulocytes and natural killer cells with anti-rat immunoglobulin-coated magnetic beads (Invitrogen) at a 7:1 bead-to-cell ratio. Immunomagnetic beads were prepared by incubation with rat anti-mouse monoclonal antibodies conjugated against the lineage defining markers CD3, CD19, CD105, TER119 and Ly6G. Lineage depleted cell suspensions were sorted for monocytes using a $CD11b^+$ $CD115^+$ $Flt3^-$ $cKit^-$ $Lineage^-$ gating strategy. Monocyte preparations had a purity of greater than 90% as measured by post-sorting flow cytometry. Cells were sorted on a FACS Aria Fusion or an Aria II flow cytometer (BD).

Bone-marrow-derived Macrophage Culture

Femurs and tibia were removed from CD45.1 wild-type or CD45.2 wild-type, $Msln^{-/-}$, or $Muc16^{-/-}$ mice and flushed with FACS to remove the bone-marrow. Bone-marrow cells were pelleted, resuspended with RPMI (Gibco) + 10% FBS + 20ng/mL M-CSF (Biolegend), seeded onto untreated petri dishes, and cultured for 6 days. Cells were removed mechanically by scratching into 1x PBS before adoptive transfer experiments.

Adoptive Transfer

For the transfer experiment, $2X10^5$ cells were injected intraperitoneally into the recipient mouse and collected 12 days later for flow cytometric analysis.

Peritoneal Lavage Preparation and Treatment on LPM

Mice were injected intraperitoneally with 2 ml of DMEM (Sigma) supplemented with 1% penicillin–streptomycin (Sigma). After gently massaging the mouse for 30 seconds, the lavage fluid was removed, centrifuged at 1500 rpm and 4˚C for 5 min, and the cell-free supernatant was collected for further experiments. Lavage fluids were boiled to denature proteins by incubation at 95˚C for 10 min.

***Ex Vivo* Stimulation**

For experiments requiring culturing, 200,000 sorted LPMs were seeded onto tissue-culture treated 96-well plates and maintained in DMEM + 1% penicillin-streptomycin. Cells that were to be used as no-culture controls were fixed immediately after sorting using 4% (v/v) paraformaldehyde and kept until analysis. Cells in experimental groups were cultured for 24hrs before harvesting for protein analysis or for 6hrs before qRT-PCR analysis. In experiments with the blockade of Msln,

LPMs were treated with un-fractioned peritoneal lavage fluid plus either 25μg/ml Msln blocking or isotype control antibodies (Antibody 1: MBL and Antibody 2: Abbiotec) for 24 hours before collection. Amicon Ultra-15 100K MWCO (Millpore) was used to size fractionate the peritoneal lavage fluid according the manufacturer's protocol.

Quantitative Real-Time Polymerase Chain Reaction (qRT-PCR)

RNA was isolated from sorted LPMs with the NucleoSpin RNA kit (Macherey-Nagel), and cDNA was synthesized with iScript cDNA kit (Bio-Rad). qRT-PCR was performed with TB Green qPCR premix (Clontech) using an Eppendorf Master-cycler. Relative expression levels were normalized to *Hprt* which was expressed at similar levels in all samples. The following primers were used: *Hprt*, forward 5′-TCAGTCAACGGGGGACATAAA-3′, reverse 5′-GGGGCTGTACTGCTTA ACCAG-3′; *Gata6* forward 5'- TTGCTCCGGTAACAGCAGTG-3' reverse 5'- GTGGTCG CTTGTGTAGAAGGA-3'. *Cebpb* forward 5'-GGAGACGCAGCACAAGGT-3' reverse 5'- AGCTG CTTGAACAAGTTCCG-3'; *Bhlhe40* forward 5'- CGTTGAAGCACGTGAAAGCA-3' reverse 5'- TCCCGACAAATCACCAGCTT-3'; *Rarb* forward 5'- ACATGATCTACACTTGC CATCG-3' reverse 5'- TGAAGGCTCCTTCTTTTTCTTG-3'; *Nfe2* forward 5'- TCCTCAGCA GAACAGGAA CAG-3' reverse 5'- GGCTCAAAAGATGTCTCACTTGG-3'.

Primary Peritoneal Mesothelial Cell Isolation

Mesothelial cells for RNA sequencing were isolated from 8 to 12 week-old wild-type or *Msln*$^{-/-}$ mice using a previously described protocol[142]. Briefly, mice were sacrificed, and their peritoneal cavities were exposed. The peritoneal cavities were washed with injecting 10 ml of 1x PBS (Sigma) via a syringe equipped with a 25G×5/8″ needle (BD). After gently shaking for 30 seconds,

the fluid was removed and discarded. The peritoneum was filled with 5 ml of 0.25% Trypsin/EDTA solution (Gibco). The corpse was then maintained at 37°C for 20 min in a tissue-culture incubator before removal of the fluid. The detached cells were pelleted by centrifugation at 300×g for 10 min and resuspended in FACS buffer. The mesothelial cells were sorted from the cell suspension as $CD45^{-}$ $PDPN^{+}$ $GPM6a^{+}$ cells into DMEM + 10% FBS on a FACS Aria II flow cytometers (BD).

RNA-sequencing and Analysis

Primary mesothelial cells were collected from 10 week old mice as mentioned above. Total RNA was extracted using NucleoSpin RNA kit (Macherey-Nagel). RNA-sequencing libraries from peritoneal mesothelial cells were generated and sequenced at the Genome Technology Access Center (GTAC) at Washington University. Pooled libraries were sequenced on an Illumina HiSeq 2500 using 1x50 single end sequencing. Transcript abundance was estimated using Kallisto software [143] and the Gencode M14 annotation (GRCm38.p5 assembly). Transcript abundances were summarized at the gene-level using the R package tximport (Soneson), and then pre-processed and normalized using packages edgeR and Limma (Robinson, Ritchie). Raw sequence data from published studies of murine large peritoneal macrophages and inguinal adipose tissue was downloaded from the NCBI Short Reads Archive. Transcript abundance was estimated and summarized in an identical fashion. Differential expression testing was performed with Limma, using cut-off values 10^{-4} for adjusted p-value and 4 for log2 fold change.

Msln and TNFα ELISA

Peritoneal lavage was prepared from naïve wild-type and $Msln^{-/-}$ mice as described above and measured for Msln concentration using a Msln ELISA kit (Abcam) according to manufacturer's instructions. . For TNFα ELISA, peritoneal exudate cells were prepared from naive wild-type and *Msln*$^{-/-}$ or *Muc16*$^{-/-}$ mice. 200,000 cells were seeded onto tissue-culture treated 96-well plates and stimulated with 1µg/ml LPS in DMEM + 10% FBS for 24 hours. Supernatant was measured for TNFα concentration using a TNFα ELISA kit (Biolgend) according to manufacturer's instructions. The signals were measured by Cytation 5 (Biotek).

In situ Hybridization

Tissues were fixed in 4% (v/v) paraformaldehyde at 4ºC for 18 to 24 hours, dehydrated with 20% sucrose in 1x PBS, and embedded in OCT (Sakura Finetek). Tissue sections were cut at a thickness of 5 µm and were used for RNAscope based in situ hybridization according to the protocols recommended by the manufacturing company (Advanced Cell Diagnostics). The RNAscope probes used were Mm-MSLN and Mm-MUC16.

Zymosan-induced Peritonitis

Peritonitis was induced by intraperitoneal injection of $2x10^6$ zymosan particles (Sigma). Peritoneal exudate cells were collect by peritoneal lavage as described earlier after 3 hours or 7 days as indicated.

Bone Marrow Chimeras

Recipient CD45.1 or CD45.2 mice were lethally irradiated with a single dose of 1050 rads from a gamma irradiator and after an overnight rest period were reconstituted intravenously with 10

million bone-marrow cells from the indicated donor animals. Mice were allowed to reconstitute their hematopoietic compartment for at least 8 weeks before experimentation.

Statistical Analysis

All data are from at least two independent experiments, unless otherwise indicated. Pairwise comparison data were analyzed by unpaired two-tailed Mann-Whitney U-tests. Statistical significance between multiple groups was evaluated by one-way ANOVA followed by Tukey's multiple comparisons post-hoc test. Data analysis was conducted in Prism 8 (GraphPad Software, Inc.). A p-value of less than or equal to 0.05 was considered significant.

Data Availability

The data that support the findings of this study are available from the corresponding author upon request. The RNA sequencing data are deposited under the GEO repository accession codes GSE 129391.

Chapter 2: Result

Mesothelium-derived protein Msln and Mucin 16 sustains Gata6 expression in LPMs

LPMs require Gata6 expression for maintenance of their function[40,134,135]. Addition of retinoic acid to LPMs *in vitro* can stimulate a detectable increase in Gata6 expression in LPMs[40,127]. Using this experimental system, we cultured sorted LPMs ($FSC^{lnt}CD11b^{+}ICAM2^{+}F4/80^{+}$) in serum-free media and found that Gata6 protein expression in LPMs was not maintained after 24 hours of culture (**Fig 1A-C**). Under these experimental conditions, we found that additional treatment of LPMs with peritoneal lavage fluid from wild-type (WT) mice could partially preserve Gata6

protein levels in LPMs. This activity appeared to be due to protein factor(s) as heat denaturation diminished the effect of the peritoneal lavage fluid in this assay. The effects of the peritoneal lavage fluid similarly affected *Gata6* mRNA expression after 6 hours of culture (**Fig 1D)**.

Due to their immediate proximity to the peritoneal cavity, we propose that mesothelial cells can produce and secrete proteins into the peritoneum[144] to maintain Gata6 expression by LPMs. We used comparative transcriptomics to identify secreted factors that were specifically and highly expressed in primary mesothelium. We performed bulk RNA-sequencing of mesothelial cells from 10 week old healthy mice. Using publicly available data-sets from healthy mice, we identified genes that were expressed at significantly greater levels in mesothelial cells as compared to two other peritoneal cell types, adipocytes and LPMs[127,145]. Transcripts from 315 genes were significantly enriched in mesothelial cells using cut-off values 10^{-4} for adjusted p-value and 4 for log2 fold change. As expected, this list included known mesothelial markers including *Wt1* and *Gpm6a.* Two genes, *Msln* and *Muc16*, were among the most highly enriched genes that were predicted to be secreted from mesothelial cells (**Fig. 1E and Supplementary Fig 1A**).

One candidate, Msln was of interest as it is specifically expressed by mesothelial cells[146] and not immune cells in the peritoneal cavity (**Supplementary Fig 1B, C**), and it has been shown by previous work to be a secreted protein[147-150]. In addition, *in vivo* and *in vitro* tools have been developed previously to study its function[151]. Using the model of cultured LPMs as above, we blocked Msln function by mixing the lavage fluid from WT mice with Msln blocking antibodies. We used two antibodies that recognize different epitopes of Msln and both antibodies inhibited the

maintenance of Gata6 expression in isolated and cultured LPMs while isotype controls had no detectable effect (**Fig. 1F, G**).

We next evaluated the expression of Msln. By ELISA, we detected Msln protein in peritoneal lavage fluid of WT but not *Msln*$^{-/-}$ mice (**Fig. 1H**). Because a mature 30kD Msln protein has been described to function in a complex with other proteins such as Muc16 (MW >250kDa), we performed size selection on the peritoneal lavage fluid from WT mice and found proteins in a fraction >100kD contained the majority of Msln while the smaller sized fraction (<100kD) contained lower levels of Msln. We found that the >100kDa fraction contained the activity required to preserve Gata6 expression at an RNA and protein level (**Fig. 1I, J**). Muc16 has been proposed to be a co-factor for Msln in cancer cells [98,152] and is known to have a secreted form [153]. Similar to Msln, it is specifically expressed by mesothelial cells but not immune cells (**Supplementary Fig 1D, E**). These data create the hypothesis that Msln and Muc16 produced by mesothelial cells are important local factors for the preservation of the expression of the transcription factor Gata6 in LPMs, suggesting a possible role that is similar to a previously described role for retinoic acid [40,127]. Our results show that proteins (Msln and Mucc16) in the peritoneal fluid can maintain Gata6 expression in *ex vivo* cultured LPMs.

Msln $^{-/-}$ **mice have lower expression of specific markers of LPMs**

We analyzed LPMs and other immune cells in the peritoneal cavities in *Msln*$^{-/-}$ and *Msln*$^{+/+}$ littermate control adult mice. The number of LPMs was similar in *Msln*$^{-/-}$ mice and controls (**Supplementary Fig 2A**). However, the Gata6 and F4/80 levels of expression of LPMs isolated from *Msln*$^{-/-}$ mice were lower than controls (**Fig 2A-E**). Macrophages in the lung pleural space of

Msln$^{-/-}$ mice also showed lower levels of Gata6 and F4/80 expression as compared to littermate controls (**Fig 2F-H**). To determine if Msln has an effect on peritoneal cavity inflammation, we injected zymosan into the peritoneal cavity of mice which induces neutrophil infiltration in WT mice within 3 hours[46]. *Msln*$^{-/-}$ mice had increased neutrophil infiltration in response to zymosan injection as compared to littermate controls and this effect was comparable to the effects of zymosan injection into Gata6 conditional knockout in macrophages (*Gata6*$^{f/f}$, LysM-Cre) mice[135] (**Fig 2I**). We also used zymosan treatment to stimulate the loss of macrophages in the peritoneal space and to study macrophage repopulation from blood derived monocytes[154]. As expected, >99% of LPMs were no longer detected in the peritoneal lavage of treated WT and *Msln*$^{-/-}$ mice after 3 hours of zymosan treatment [46]. We found that in zymosan treated *Msln*$^{-/-}$ mice, the LPMs that repopulated the peritoneal cavity had a lower proportion of Gata6-positive, F4/80-positive cells as compared to similarly treated WT littermates (**Fig 2J-L**). This finding suggests that Msln can influence TRM identity in mesothelium-lined compartments at both the steady state and during inflammation.

To investigate the effects of Msln on LPMs during development, we analyzed immune cells from the peritoneal cavity of two week old littermate WT and *Msln*$^{-/-}$ mice. Surprisingly, the expression of F4/80 and Gata6 in LPMs from *Msln*$^{-/-}$ mice was comparable to WT controls (**Supplementary Fig 2B, C**). The percentage of Gata6 and F4/80 low LPMs in two-week old *Msln*$^{-/-}$ mice was also comparable to controls, suggesting that Msln affects LPM identity after this developmental time period. Using LPMs in adult *Msln*$^{-/-}$ naïve mice, we found no defects in LPM proliferation (Ki67^{+}) or cell death (AnnexinV^{+}PI^{+}) (**Supplementary Fig 2D, E**). Amongst the other immune populations of peritoneal exudate cells, splenocytes, and lymphoid cells in Peyer's

Patches, we observed no difference in the abundance of these cells in *Msln*$^{-/-}$ mice (**Supplementary Fig 2F-J**). These results were replicated in a second facility with a distinct microbiome[155], suggesting that this phenotype is not dependent on differences in gut microbes (**Supplementary Fig 2K**). We also examined *Gata6* and other LPM-related gene expression in LPM by qRT-PCR and found that Msln deficiency affected not only *Gata6* but also *Bhlhe40*, a tissue-specific transcriptional regulator of LPM proliferation[156] (**Supplementary Fig 2L**). Overall, we found that adult *Msln*$^{-/-}$ mice have abnormal TRMs in mesothelium-lined compartments and these cells express lower levels of identity defining markers Gata6 and F4/80.

Msln acts extrinsically on Gata6 expression during TRM differentiation in bone marrow chimeras

Based on these findings, we hypothesized that Msln produced by mesothelial cells acts locally in the peritoneal cavity to influence Gata6 expression in LPMs and that continuous exposure of LPMs to Msln is needed for optimal expression of Gata6. We first excluded a developmental role for Msln in bone marrow (BM), as both WT and *Msln*$^{-/-}$ mice had similar numbers of common monocyte progenitors (cMoPs)[157] (**Fig 3A**). We next reconstituted irradiated WT and *Msln*$^{-/-}$ CD45.2 mice with WT CD45.1 bone marrow in order to determine extrinsic versus intrinsic effects of Msln. The CD45.1 macrophages expressed less Gata6 in *Msln*$^{-/-}$ recipient mice as compared to WT recipients (**Fig 3B, C, Supplementary Fig 3A-C**), consistent with our model that mesothelial cells acted as an extrinsic source of Msln to impact macrophage differentiation. Additionally, analysis of 'reversed' chimeric mice excluded intrinsic effects of Msln on LPMs as BM transfer from *Msln*$^{-/-}$ CD45.2 mice into WT CD45.1 recipients had Gata6 expression in LPMs and lung

pleural macrophages that was similar to that of BM derived LPMs from littermate WT CD45.2 mice (**Fig 3D, Supplementary Fig 3D, E**).

We used a second approach to test the role of Msln on LPM Gata6 expression that did not involve irradiation needed to produce BM chimeras. Adapting a technique used to show the acquisition of the TRM features of alveolar macrophages by macrophage precursors[129], we adoptively transferred either WT monocytes or bone marrow derived macrophages (BMDMs) intraperitoneally into untreated *Msln*$^{-/-}$ or WT littermates. We then harvested peritoneal exudates 12 days post injection. The percentage of the total pool of LPMs represented by the transferred CD45.1 cells ranged from 0.5 to 1%. Further analysis of the CD45.1 transferred cells showed that they had acquired features of LPMs (ICAM2^{+}) in both *Msln*$^{-/-}$ and WT recipient mice. However, the CD45.1 LPMs in the *Msln*$^{-/-}$ recipient mice expressed less Gata6 than in WT recipients (**Fig 3E-H, Supplementary Fig 3F, G**). The percentage and absolute numbers of LPMs were comparable between WT and *Msln*$^{-/-}$ mice. Taken together, Msln acts extrinsically to modulate the expression of Gata6 in TRMs found in mesothelial cell lined cavities.

Muc16 deficiency recapitulates the effects of Msln deficiency on tissue resident macrophages

We identified both Msln and Muc16 as secreted candidates in regulating Gata6 expression in LPMs. Given its potential interaction with Msln[98,152], expression in mesothelial cells (**Fig 1E**) and high molecular weight (>2 million Da), we tested if Muc16 was also necessary for Gata6 expression in LPMs. Similar to the *Msln*$^{-/-}$ mice, the LPMs and pleural macrophages from *Muc16*$^{-/-}$ mice had lower Gata6 expression as compared to littermate controls (**Fig 4A, B, Supplementary Fig 3H, I**). Zymosan-induced peritonitis in *Muc16*$^{-/-}$ mice showed an increase in recruited

neutrophils that was similar in magnitude to *Msln*$^{-/-}$ mice (**Fig 4C**). Additionally, seven days post zymosan challenge, *Muc16*$^{-/-}$ mice contained fewer Gata6+ LPMs, similar to *Msln*$^{-/-}$ mice tested in this way (**Fig. 4D, Supplementary Fig 3J**).

We next tested whether the effect of Muc16 deficiency was extrinsic. Repopulation of *Muc16*$^{-/-}$ mice with WT bone marrow cells led to a decrease in Gata6 expression in LPMs and pleural macrophages as compared to WT recipient mice, an effect similar to repopulation of the BM in *Msln*$^{-/-}$ mice (**Fig 4E, Supplementary Fig 3K-M**). Next, analysis of 'reversed' chimeras further excluded intrinsic effects of Muc16 on LPMs as BM transfer from *Muc16*$^{-/-}$ CD45.2 mice into WT CD45.1 recipients had comparable effects on Gata6 expression in LPMs as BM from littermate WT CD45.2 mice (**Fig 4F).** After adoptively transferring CD45.1 monocytes and BMDMs, donor-derived LPMs also expressed lower F4/80 and Gata6 in the *Muc16*$^{-/-}$ recipient mice compared to WT (**Fig. 4G, H, Supplementary Fig 3N, O**). These results support a role for Muc16 in addition to Msln to promote Gata6 expression in LPMs.

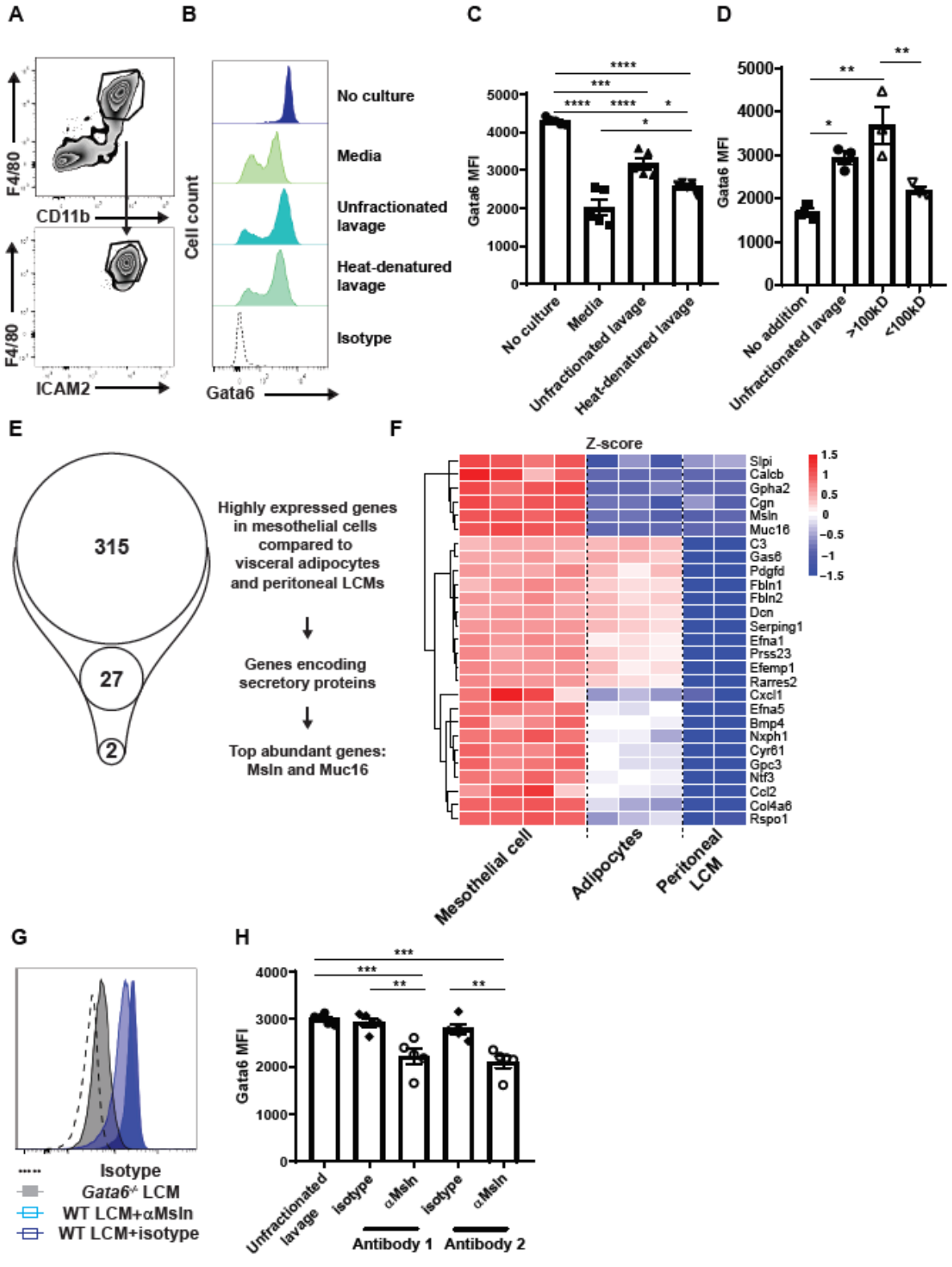
A
B
C
D
F4/80
CD11b
F4/80
ICAM2
Cell count
Gata6
No culture
Media
Unfractionated lavage
Heat-denatured lavage
Isotype
Gata6 MFI
No culture
Media
Unfractionated lavage
Heat-denatured lavage
No addition
Unfractionated lavage
>100kD
<100kD
E
315
27
2
Highly expressed genes in mesothelial cells compared to visceral adipocytes and peritoneal LCMs
Genes encoding secretory proteins
Top abundant genes: Msln and Muc16
F
Z-score
Slpi
Calcb
Gpha2
Cgn
Msln
Muc16
C3
Gas6
Pdgfd
Fbln1
Fbln2
Dcn
Serping1
Efna1
Prss23
Efemp1
Rarres2
Cxcl1
Efna5
Bmp4
Nxph1
Cyr61
Gpc3
Ntf3
Ccl2
Col4a6
Rspo1
Mesothelial cell
Adipocytes
Peritoneal LCM
G
Isotype
Gata6-/- LCM
WT LCM+αMsln
WT LCM+isotype
H
Gata6 MFI
Unfractionated lavage
Isotype
αMsln
Isotype
αMsln
Antibody 1
Antibody 2

Figure 2.1 Soluble proteins in peritoneal lavage fluid sustains Gata6 expression in LPMs

(A) Representative FACS plots of isolated LPMs ($CD11b^+F4/80^+ICAM2^+$). **(B)** Representative histograms of Gata6 expression from isolated LPMs (no culture) or LPMs cultured for 24 hours in media alone (no addition), or media lavaged in the peritoneal cavity (un-fractioned and with heat denaturation). **(C)** Average mean fluorescence intensity (MFI) ± SEM of Gata6 for the four groups of LPMs displayed in B**. (D)** Average relative expression ± SEM of *Gata6* (by qRT-PCR) for the four groups of LPMs in B except that LPMs were cultured for 6 hours. **(E)** The diagram depicting the number of genes that were expressed at significantly greater levels in isolated mesothelial cells compared to two other peritoneal cell types, adipocytes and LPMs. The number of genes making secretory proteins were generated by the gene ontology resource and literature review. **(F)** Representative histogram of Gata6 expression from WT LPMs treated with peritoneal lavage for 24 hours plus either Msln blocking or isotype control antibodies. **(G)** Average MFI ± SEM of Gata6 for the experimental design in F. Two different blocking antibodies directed against Msln (25ug/ml, Antibody 1 and Antibody 2) and their isotype controls were used. **(H)** Average expression of soluble Msln ± SEM (by ELISA) from the peritoneal lavage of WT and $Msln^{-/-}$ mice. The WT lavage was fractionated into >100kD and <100kD. Dash line labels the limit of detection. **(I)** Average MFI ± SEM of Gata6 from WT LPMs treated with unfractionated lavage and fractions >100kDa and <100kDa for 24 hours. **(J)** Average expression ± SEM of *Gata6* mRNA (by qRT-PCR) in peritoneal lavages: unfractionated and fractions >100kD and <100kD. Statistical significance in C, D, G-J determined by a one-way ANOVA followed by Tukey's multiple comparisons post hoc tests. $*P < 0.05$, $**P < 0.01$, $***P < 0.001$, $****P < 0.0001$. (N = 3 independent experiments) In E

determined by cut-off values 10^{-4} for adjusted p-value and 4 for log2 fold change to get mesothelial cell specific genes.

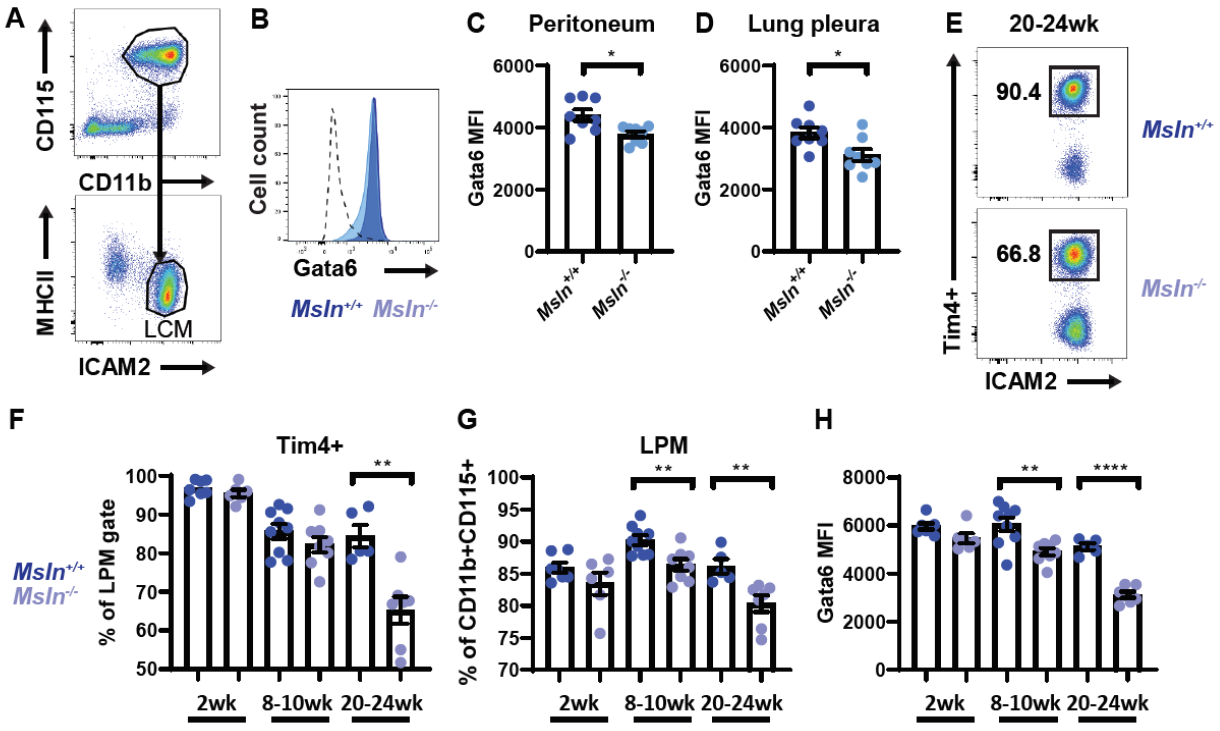
A
CD115
CD11b
MHCII
LCM
ICAM2
B
Cell count
Gata6
Msln+/+ Msln-/-
C
Peritoneum
Gata6 MFI
6000
4000
2000
0
*
Msln+/+
Msln-/-
D
Lung pleura
Gata6 MFI
6000
4000
2000
0
*
Msln+/+
Msln-/-
E
20-24wk
90.4
66.8
Msln+/+
Msln-/-
Tim4+
ICAM2
F
Tim4+
Msln+/+
Msln-/-
% of LPM gate
100
90
80
70
60
50
**
2wk
8-10wk
20-24wk
G
LPM
% of CD11b+CD115+
100
95
90
85
80
75
70
**
**
2wk
8-10wk
20-24wk
H
Gata6 MFI
8000
6000
4000
2000
0
**
****
2wk
8-10wk
20-24wk

Figure 2.2. *Msln*$^{-/-}$ mice have lower expression of specific markers of LPMs

(A) Representative FACS plots of Gata6 and F4/80 expression in isolated LPMs ($CD11b^{+}CD115^{+}MHCII^{lo}ICAM2^{+}$) from adult *Msln*$^{-/-}$ and littermate mice. **(B)** Representative histograms of Gata6 expression in LPMs from adult *Msln*$^{-/-}$ and littermate mice. **(C)** Average percentage ± SEM of Gata6+ LPMs, **(D)** average relative MFI expression ± SEM of Gata6 for LPMs, and **(E)** average percentage ± SEM of F4/80+ LPMs from adult *Msln*$^{-/-}$ and littermate mice. **(F)** Average percentage ± SEM of Gata6+ lung pleural macrophages ($CD11b^{+}CD115^{+}MHCII^{lo}ICAM2^{+}$), **(G)** average relative MFI expression ± SEM of Gata6 for lung pleural macrophages, and **(H)** average percentage ± SEM of F4/80+ lung pleural macrophages from adult *Msln*$^{-/-}$ and littermate mice. (5 pooled experiments, N = 19 to 20 mice/group). **(I)** Average number of neutrophils in the peritoneal cavity from zymosan (2×10^{6} particles) -stimulated *Msln*$^{-/-}$ and littermate 3 hours post injection (3 to 4 pooled experiments, N = 9 to 12). **(J)** Average percentage ± SEM of Gata6+ LPMs, **(K)** average relative MFI expression ± SEM of Gata6 for LPMs, and **(L)** average percentage ± SEM of F4/80+ LPMs from adult *Msln*$^{-/-}$ and littermate mice 7 days post zymosan (2×10^{6} particles) intraperitoneal injection. (3 pooled experiments, N = 11 to 14). Statistical significance in C-L determined by a two-tailed unpaired U-test. $^{**}P < 0.01$, $^{***}P < 0.001$, $^{****}P < 0.0001$.

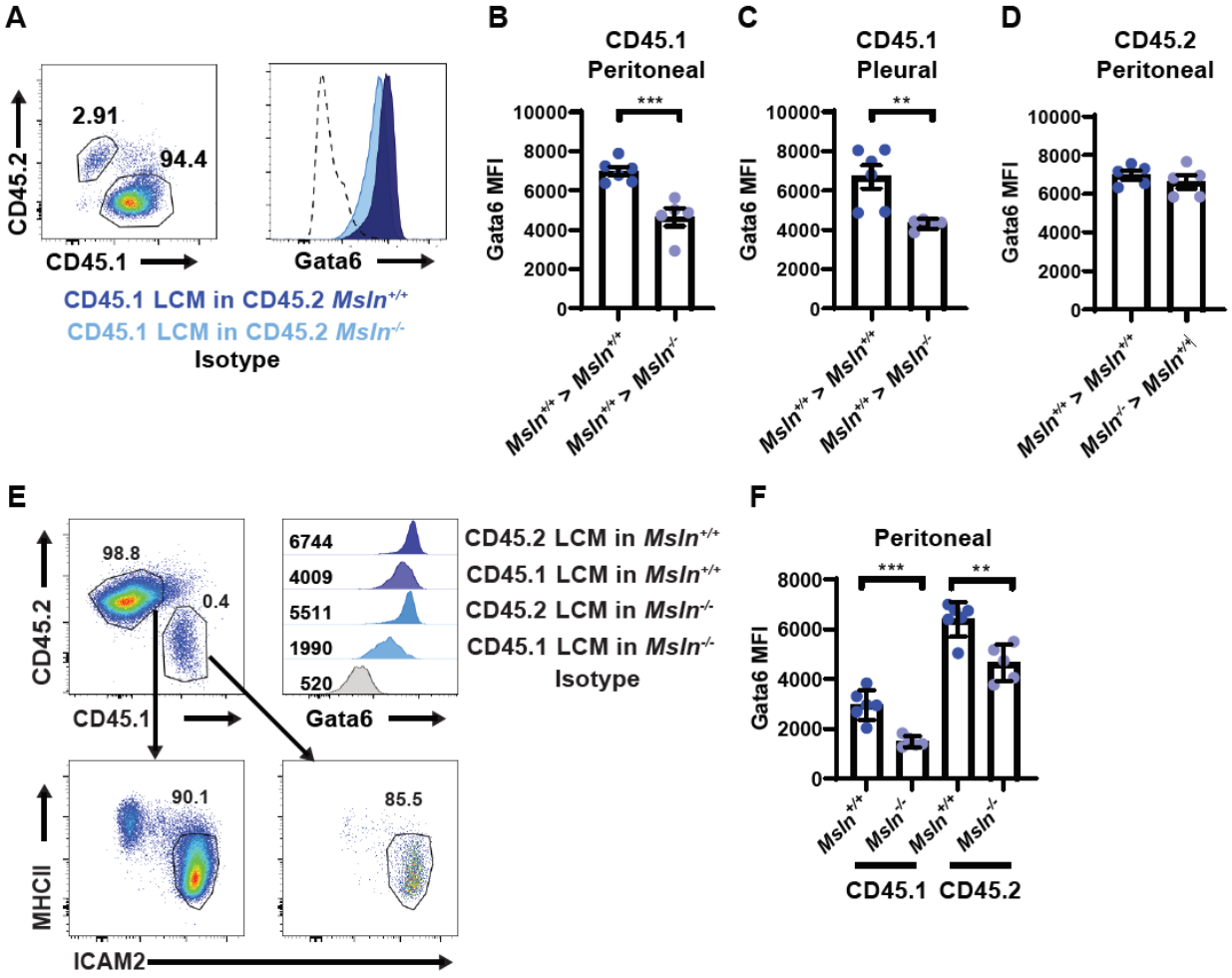
A
2.91
94.4
CD45.2
CD45.1
Gata6
CD45.1 LCM in CD45.2 Msln+/+
CD45.1 LCM in CD45.2 Msln-/-
Isotype
B
CD45.1
Peritoneal
***
Gata6 MFI
10000
8000
6000
4000
2000
0
Msln+/+ > Msln+/+
Msln+/+ > Msln-/-
C
CD45.1
Pleural
**
Gata6 MFI
Msln+/+ > Msln+/+
Msln+/+ > Msln-/-
D
CD45.2
Peritoneal
Gata6 MFI
Msln+/+ > Msln+/+
Msln-/- > Msln+/+
E
98.8
0.4
CD45.2
CD45.1
Gata6
6744
4009
5511
1990
520
CD45.2 LCM in Msln+/+
CD45.1 LCM in Msln+/+
CD45.2 LCM in Msln-/-
CD45.1 LCM in Msln-/-
Isotype
90.1
85.5
MHCII
ICAM2
F
Peritoneal
***
**
Gata6 MFI
8000
6000
4000
2000
0
Msln+/+
Msln-/-
Msln+/+
Msln-/-
CD45.1
CD45.2

Figure 2. 3. Msln acts extrinsically on Gata6 expression in the process of TRM differentiation

(A) Average number of cMoPs ($cKit^{lo}$ $Flt3^{-}$ $CD115^{+}$ $Ly6c^{hi}$ $CD11b^{+}$ $CD11c^{-}$ $Ly6G^{-}$) from *Msln*$^{-/-}$ and littermate. Data are representative of two independent experiments. **(B)** Representative histograms of Gata6 expression in CD45.1 LPMs in congenically distinct recipients (CD45.2 *Msln*$^{-/-}$ and littermate) 8 weeks after irradiation and reconstitution. **(C)** Average relative MFI expression ± SEM of Gata6 for CD45.1 LPMs from *Msln*$^{-/-}$ and littermate recipients. (3 pooled experiments, N = 10). **(D)** Average relative MFI expression ± SEM of Gata6 for CD45.2 LPMs in congenically distinct recipients (CD45.1 WT) 8 weeks after irradiation and reconstitution with *Msln*$^{-/-}$ and littermate BM. (2 pooled experiments, N = 10). **(E)** Representative FACS plots of CD45.1 LPMs ($CD11b^{+}CD115^{+}MHCII^{lo}ICAM2^{+}$) from adult CD45.2 *Msln*$^{-/-}$ and littermate mice 12 days post monocyte ($2X10^{5}$ cells per mouse) intraperitoneal injection. **(F)** Representative histograms of Gata6 expression in CD45.1 and CD45.2 LPMs displayed in E. **(G)** Average relative MFI expression ± SEM of Gata6 for CD45.1 LPMs in congenically distinct recipients (CD45.2 *Msln*$^{-/-}$ and littermate) (2 pooled experiments, N = 10). **(H)** Average relative MFI expression ± SEM of Gata6 for CD45.1 LPMs in congenically distinct recipients (CD45.2 *Msln*$^{-/-}$ and littermate) 12 days post BMDM ($2X10^{5}$ cells per mouse) intraperitoneal injection. (3 pooled experiments, N = 12 to 14). Statistical significance in C, D, G, H determined by a two-tailed unpaired U-test. $^{**}P < 0.01$, $^{****}P < 0.0001$.

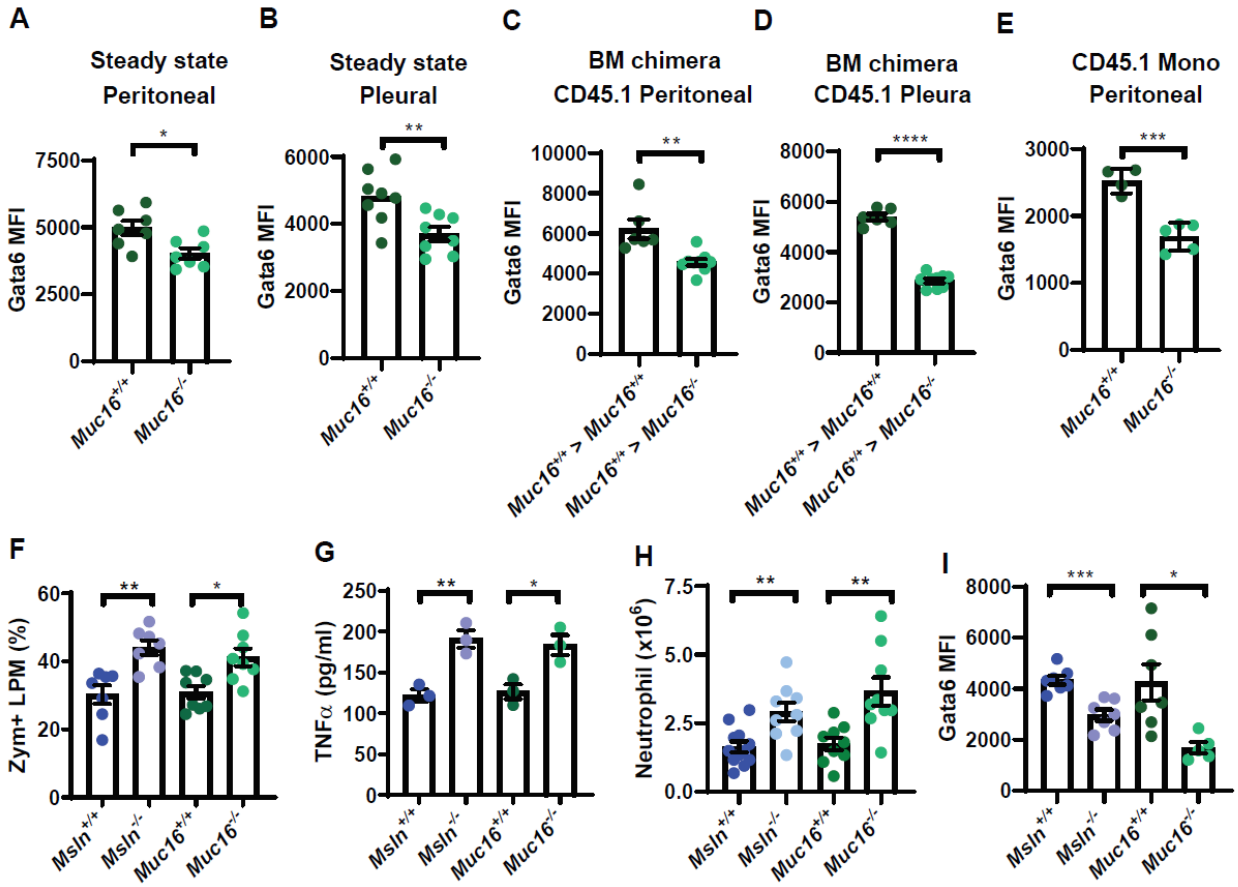
A
Steady state
Peritoneal
Gata6 MFI
7500
5000
2500
0
*
Muc16+/+
Muc16-/-
B
Steady state
Pleural
Gata6 MFI
6000
4000
2000
0
**
Muc16+/+
Muc16-/-
C
BM chimera
CD45.1 Peritoneal
Gata6 MFI
10000
8000
6000
4000
2000
0
**
Muc16+/+ > Muc16+/+
Muc16+/+ > Muc16-/-
D
BM chimera
CD45.1 Pleura
Gata6 MFI
8000
6000
4000
2000
0
****
Muc16+/+ > Muc16+/+
Muc16+/+ > Muc16-/-
E
CD45.1 Mono
Peritoneal
Gata6 MFI
3000
2000
1000
0
***
Muc16+/+
Muc16-/-
F
Zym+ LPM (%)
60
40
20
0
**
*
Msln+/+
Msln-/-
Muc16+/+
Muc16-/-
G
TNFα (pg/ml)
250
200
150
100
50
0
**
*
Msln+/+
Msln-/-
Muc16+/+
Muc16-/-
H
Neutrophil (x10^6)
7.5
5.0
2.5
0.0
**
**
Msln+/+
Msln-/-
Muc16+/+
Muc16-/-
I
Gata6 MFI
8000
6000
4000
2000
0
***
*
Msln+/+
Msln-/-
Muc16+/+
Muc16-/-

Figure 2. 4. Muc16 deficiency recapitulates the effects of Msln deficiency on resident macrophages

(A) Average relative MFI expression ± SEM of Gata6 for LPMs and **(B)** average relative MFI expression ± SEM of Gata6 for lung pleural macrophages from adult *Muc16*$^{-/-}$ and littermate mice. (3 to 5 pooled experiments, N = 25 to 31). **(C)** Average number of neutrophils in the peritoneal cavity from zymosan (2×10^6 particles)-stimulated *Muc16*$^{-/-}$ and littermate 3 hours post injection (3 pooled experiments, N = 9). **(D)** Average relative MFI expression ± SEM of Gata6 for LPMs from adult *Muc16*$^{-/-}$ and littermate mice 7 days post zymosan (2×10^6 particles) intraperitoneal injection. **(E)** Average relative MFI expression ± SEM of Gata6 for CD45.1 LPMs from *Muc16*$^{-/-}$ and littermate recipients 8 weeks after irradiation and reconstitution. (3 pooled experiments, N = 10). **(F)** Average relative MFI expression ± SEM of Gata6 for CD45.2 LPMs in congenically distinct recipients (CD45.1 WT) 8 weeks after irradiation and reconstitution with *Muc16*$^{-/-}$ and littermate BM. (2 pooled experiments, N = 10). **(G)** Average relative MFI expression ± SEM of Gata6 for CD45.1 LPMs in congenically distinct recipients (CD45.2 *Msln*$^{-/-}$ and littermate) 12 days post monocytes ($2X10^5$ cells per mouse) intraperitoneal injection. (2 pooled experiments, N = 7 to 9) **(H)** Average relative MFI expression ± SEM of Gata6 for CD45.1 LPMs in congenically distinct recipients (CD45.2 *Msln*$^{-/-}$ and littermate) 12 days post BMDM ($2X10^5$ cells per mouse) intraperitoneal injection. (3 pooled experiments, N = 7 to 11). Statistical significance in A-H determined by a two-tailed unpaired U-test. $^{**}P < 0.01$, $^{***}P < 0.001$, $^{****}P < 0.0001$.

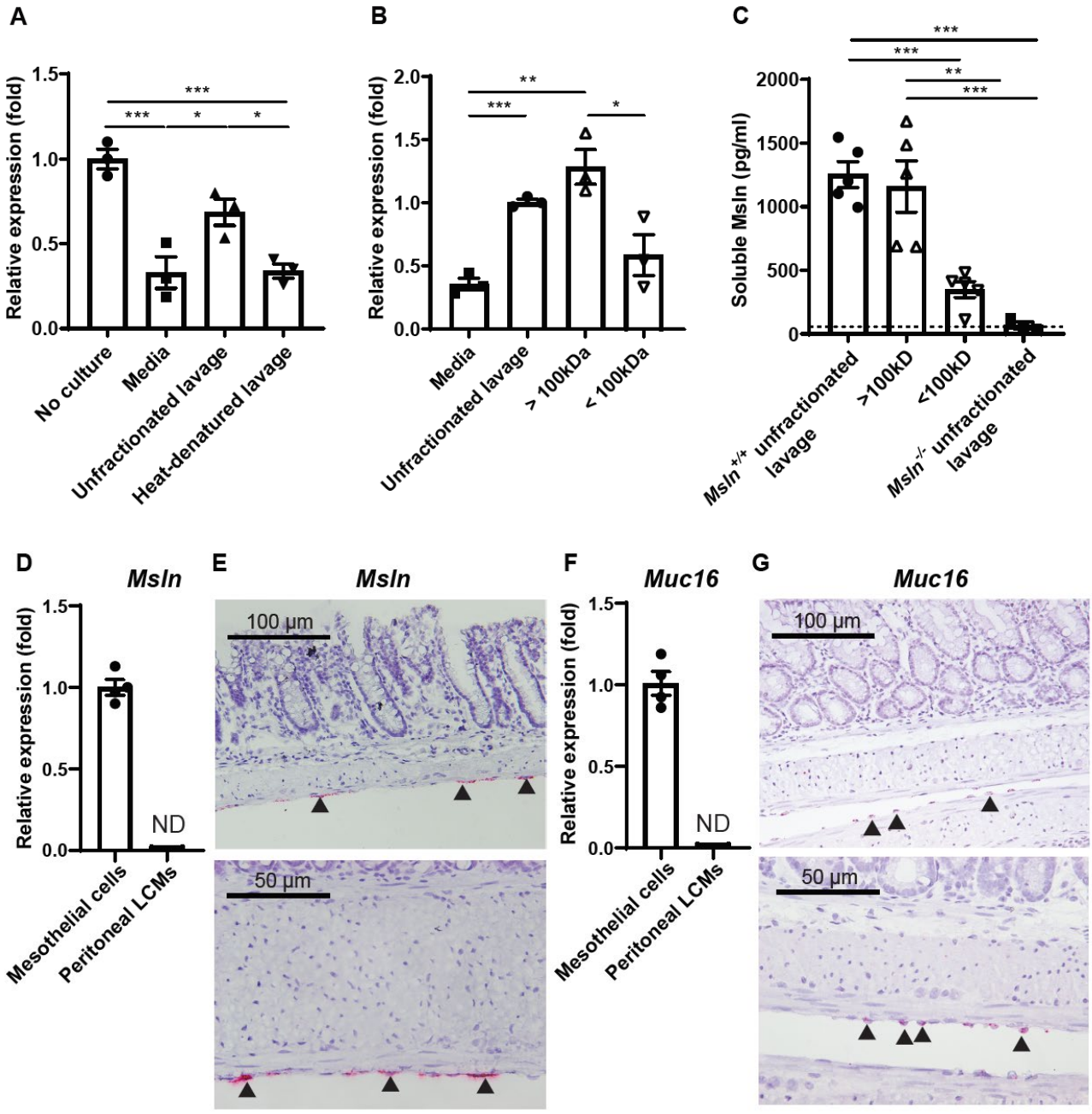
A
Relative expression (fold)
1.5
1.0
0.5
0.0
***
***
*
*
No culture
Media
Unfractionated lavage
Heat-denatured lavage
B
Relative expression (fold)
2.0
1.5
1.0
0.5
0.0
**
***
*
Media
Unfractionated lavage
> 100kDa
< 100kDa
C
Soluble Msln (pg/ml)
2000
1500
1000
500
0
***
***
**
***
Msln +/+ unfractionated lavage
>100kD
<100kD
Msln -/- unfractionated lavage
D
Msln
Relative expression (fold)
1.5
1.0
0.5
0.0
ND
Mesothelial cells
Peritoneal LCMs
E
Msln
100 µm
50 µm
F
Muc16
Relative expression (fold)
1.5
1.0
0.5
0.0
ND
Mesothelial cells
Peritoneal LCMs
G
Muc16
100 µm
50 µm

Supplementary Figure 1. Msln and Muc16 expression in peritoneal mesothelial cells and LPMs

(A) 29 genes making secretory proteins among 315 mesothelial cell specific genes. **(B)** Average relative expression ± SEM of *Msln* (by qRT-PCR) in LPMs and isolated peritoneal mesothelial cells. **(C)** Representative RNA scope images for *Msln* in fresh-frozen intestine section. Black arrowheads indicate *Msln*-positive mesothelial cells. **(D)** Average relative expression ± SEM of *Muc16* (by qRT-PCR) in LPMs and isolated peritoneal mesothelial cells. **(E)** Representative RNA scope images for *Muc16* in fresh-frozen intestine section. Black arrowheads indicate *Muc16*-positive mesothelial cells. Statistical significance in B, D determined by a two-tailed unpaired U-test. ND: non-detectable.

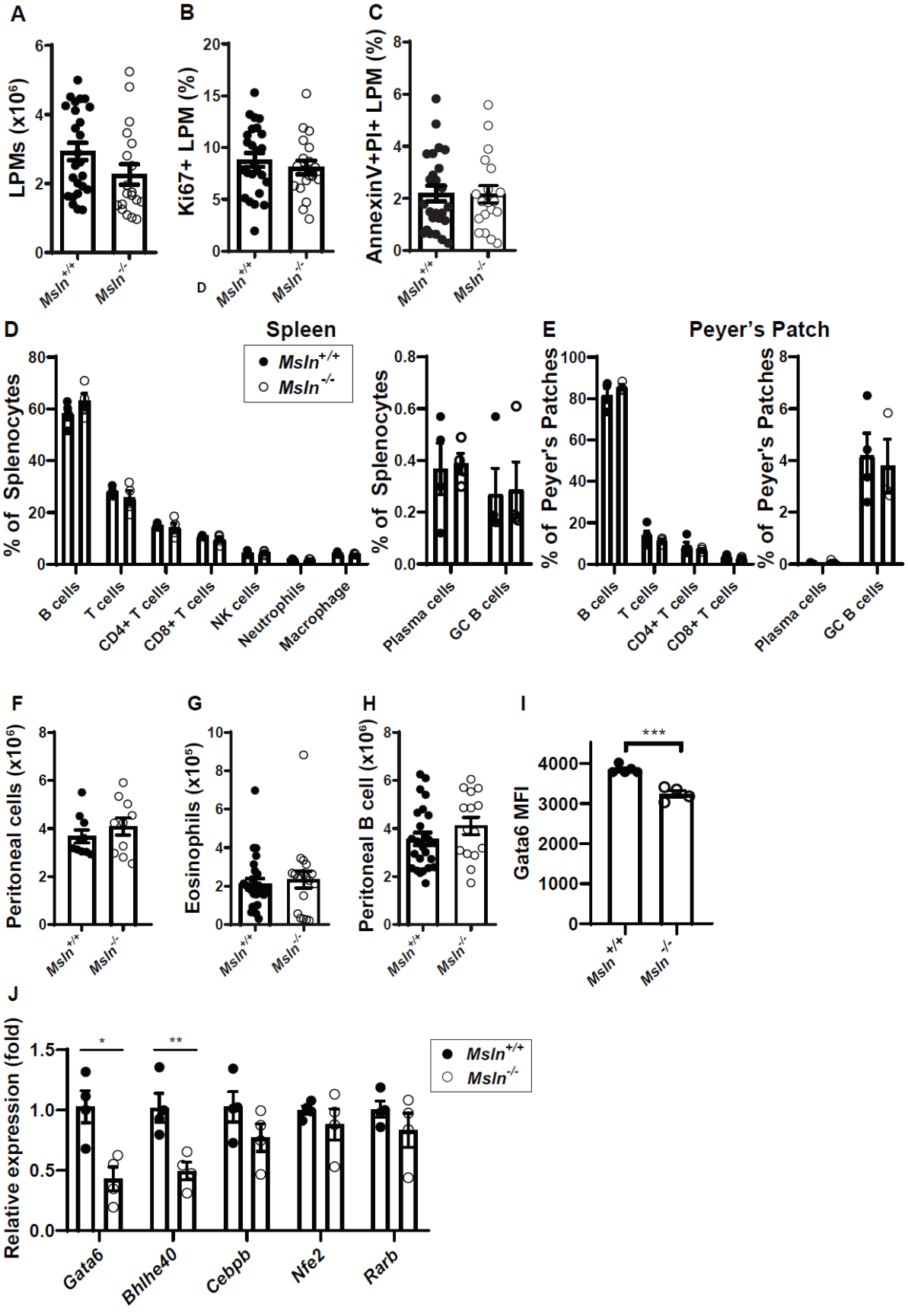
A
LPMs (x10⁶)
Msln+/+
Msln-/-
B
Ki67+ LPM (%)
C
AnnexinV+PI+ LPM (%)
D
Spleen
Msln+/+
Msln-/-
% of Splenocytes
B cells
T cells
CD4+ T cells
CD8+ T cells
NK cells
Neutrophils
Macrophage
Plasma cells
GC B cells
E
Peyer's Patch
% of Peyer's Patches
F
Peritoneal cells (x10⁶)
G
Eosinophils (x10⁵)
H
Peritoneal B cell (x10⁶)
I
Gata6 MFI
***
J
Relative expression (fold)
*
**
Gata6
Bhlhe40
Cebpb
Nfe2
Rarb

Supplementary Figure 2. The impact of Msln is restrict to tissue resident macrophages

(A) Average number of LPM from *Msln*$^{-/-}$ and littermate (5 to 7 pooled experiments, N = 20 to 25). **(B)** Average relative MFI expression ± SEM of Gata6 for LPMs and **(C)** average percentage ± SEM of F4/80+ LPMs from 2-week-old *Msln*$^{-/-}$ and littermate mice. (3 pooled experiments, N = 15). **(D)** Average percentage ± SEM of Ki67+ LPMs and **(E)** AnnexinV+PI+ LPMs from adult *Msln*$^{-/-}$ and littermate (5 to 7 pooled experiments, N = 23). **(F, G)** Average percentage ± SEM of immune cell populations in spleen, Peyer's patches from small intestine from adult *Msln*$^{-/-}$ and littermate. (2 pooled experiments, N = 4 to 10) (**H-J)** Average number ± SEM of total peritoneal exudate cells, peritoneal eosinophils, and peritoneal B cells from adult *Msln*$^{-/-}$ and littermate. (3 to 5 pooled experiments, N = 10 to 26). **(K)** Average relative MFI expression ± SEM of Gata6 for LPMs from adult *Msln*$^{-/-}$ and littermate mice in the other facility. (3 to 5 pooled experiments, N = 11 to 14) in different facility. **(L)** Average relative expression ± SEM of *Gata6, Bhlhe40, Cebpb, Nfe2, and Rarb* (by qRT-PCR) for LPMs from adult *Msln*$^{-/-}$ and littermate mice. (2 5 pooled experiments, N = 4) Statistical significance in A-L determined by a two-tailed unpaired U-test. *$P < 0.05$, **$P < 0.01$, ****$P < 0.0001$.

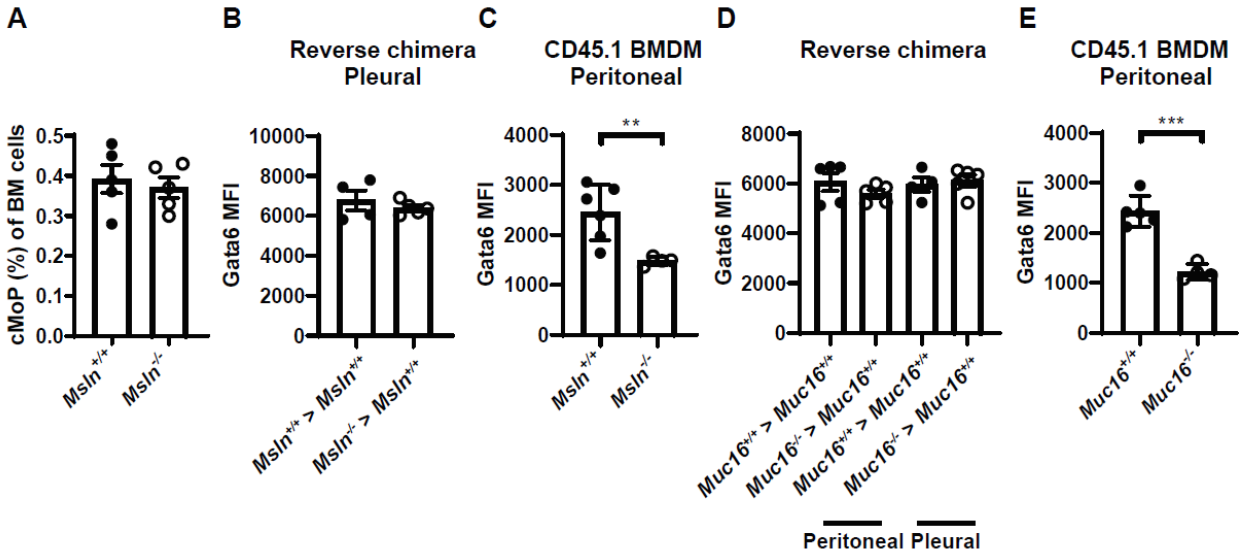
A
cMoP (%) of BM cells
0.5
0.4
0.3
0.2
0.1
0.0
Msln+/+
Msln-/-
B
Reverse chimera
Pleural
Gata6 MFI
10000
8000
6000
4000
2000
0
Msln+/+ > Msln+/+
Msln-/- > Msln+/+
C
CD45.1 BMDM
Peritoneal
Gata6 MFI
4000
3000
2000
1000
0
**
Msln+/+
Msln-/-
D
Reverse chimera
Gata6 MFI
8000
6000
4000
2000
0
Muc16+/+ > Muc16+/+
Muc16-/- > Muc16+/+
Muc16+/+ > Muc16+/+
Muc16-/- > Muc16+/+
Peritoneal
Pleural
E
CD45.1 BMDM
Peritoneal
Gata6 MFI
4000
3000
2000
1000
0
***
Muc16+/+
Muc16-/-

Supplementary Figure 3. Mice with Muc16 deficieny phenocopies mice lacking of Msln

(A) Average percentage ± SEM of Gata6+ CD45.1 LPMs from *Msln*$^{-/-}$ and littermate recipients 8 weeks after irradiation and reconstitution. (3 pooled experiments, N = 10). **(B)** Average percentage ± SEM of Gata6+ CD45.1 lung pleural macrophages and **(C)** average percentage ± SEM of Gata6+ CD45.1 lung pleural macrophages from A. (3 pooled experiments, N = 10). **(D)** Average percentage ± SEM of Gata6+ CD45.2 lung pleural macrophages and **(E)** average percentage ± SEM of Gata6+ CD45.2 lung pleural macrophages in congenically distinct recipients (CD45.1 WT) 8 weeks after irradiation and reconstitution with *Msln*$^{-/-}$ and littermate BM. (3 pooled experiments, N = 10) **(F)** Average percentage ± SEM of Gata6+ CD45.1 LPMs in congenically distinct recipients (CD45.2 *Msln*$^{-/-}$ and littermate) 12 days post monocyte (2X10^5 cells per mouse) intraperitoneal injection. **(G)** Average percentage ± SEM of Gata6+ CD45.1 LPMs in congenically distinct recipients (CD45.2 *Msln*$^{-/-}$ and littermate) 12 days post BMDM (2X10^5 cells per mouse) intraperitoneal injection. (3 pooled experiments, N = 12 to 14). **(H, I)** Average percentage ± SEM of Gata6+ LPMs and average percentage ± SEM of Gata6+ pleural macrophages from adult *Muc16*$^{-/-}$ and littermate mice. (3-5 pooled experiments, N = 25 to 31). **(J)** Average percentage ± SEM of Gata6+ LPMs from adult *Muc16*$^{-/-}$ and littermate mice 7 days post zymosan (2×10^6 particles) intraperitoneal injection. (3 pooled experiments, N = 11 to 12). **(K)** Average percentage ± SEM of Gata6+ CD45.1 LPMs from *Msln*$^{-/-}$ and littermate recipients 8 weeks after irradiation and reconstitution. (3 pooled experiments, N = 10). **(L)** Average percentage ± SEM of Gata6+ CD45.1 lung pleural macrophages and **(M)** average percentage ± SEM of Gata6+ CD45.1 lung pleural macrophages from K. (3 pooled experiments, N = 10) **(N)** Average percentage ± SEM of Gata6+ CD45.1 LPMs in congenically distinct recipients (CD45.2 *Muc16*$^{-/-}$ and littermate) 12 days post monocyte (2X10^5 cells per mouse)

intraperitoneal injection. **(O)** Average percentage ± SEM of Gata6+ CD45.1 LPMs in congenically distinct recipients (CD45.2 *Muc16*$^{-/-}$ and littermate) 12 days post BMDM (2X10^5 cells per mouse) intraperitoneal injection. (3 pooled experiments, N = 7 to 11). Statistical significance in A-O determined by a two-tailed unpaired U-test. $^{**}P < 0.01$, $^{***}P < 0.001$, $^{****}P < 0.0001$.

Chapter 2: Discussion

Local environment determines the identity of tissue resident macrophages. Here we show that, in the pleural and peritoneal cavities, Msln and Muc16 derived from mesothelial cells modulates the expression of Gata6 in macrophage precursors in an extrinsic manner and has functional consequences in acute peritonitis.

Our results highlight the potential for a potential interaction between Msln and Muc16. In cancer biology, Msln expression is elevated in several tumor types and is associated with increased tumor invasion and poor clinical outcome[151]. However, its role outside of cancer biology is less well-defined, in part because mice lacking *Msln* were not found to display a phenotype in homeostasis [88]. As a membrane-anchored glycosylphosphatidyl inositol–linked 71-kDa membrane protein (Msln precursor), Msln is proteolitically cleaved to generate mature Msln (40 kDa) and MPF (30 kDa) that is secreted from the cells[147-150].

Msln is known to bind the cell-surface protein Mucin 16 (Muc16) in an N-glycosylation dependent manner. Muc16 is a membrane spanning mucin that is expressed on ovarian, endometrial, tracheal, and ocular surface epithelial cells[158-160]. This mucin is initially expressed on the surface and then shed in the extracellular milieu following proteolytic cleavage[153]. Individually, Msln and Muc16 are biomarkers for peritoneal and tumor metastases[98,152,161]. Despite their influence on tumorigenesis, we have a poor understanding of the role of Msln and Muc16 in shaping the microenvironment in the peritoneum and other mesothelium-containing tissues for myeloid cell differentiation. Given that Muc16-Msln is thought to be ligand-receptor combination, we examined the effect of Muc16 deficiency on mesothelial-associated TRM identity and found that mice with loss of Muc16 phenocopied *Msln*$^{-/-}$ mice.

The nature of the Msln/Muc16 interaction is still unclear. Previous studies have indicated their shedding from mesothelium[84], while our data suggests that these may form a high molecular complex. Additionally, the receptor and signaling mechanism in LPMs that leads to the effect of Msln and Muc16 on Gata6 expression remains to be identified. Other than the interaction between Msln and Muc16, CD206 (Mannose receptor, Mrc1) has been reported to engage with Msln and Muc16[162,163]. One of the features of *Gata6*$^{f/f}$, LysM-Cre mice is CD206 positivity of LPMs[134], and in this study we found more CD206+ LPMs in *Msln*$^{-/-}$ and *Muc16*$^{-/-}$ animals (data not shown). Whether there is a direct interaction between CD206 and Msln/Muc16 remains to be studied. Another candidate Msln/Muc16 receptor is sialic acid binding Ig-like lectin E (Siglec-E). Siglec-9, the human Siglex-E homologue, has be identified as the immune cell receptor for MUC16 in human NK cells and monocytes[164-166]. Siglec-E changes phosphorylation of Syk and p38 mitogen-activated protein kinase in neutrophils and phosphorylation of Syk in macrophage-mediated inflammatory responses and diseases[167]. The exact receptor will need to be determined in future studies.

Monocytes extravasate through mesothelium into peritoneum in a CCR2-dependent manner[168] and become macrophages[42,169]. In homeostasis, most LPMs are derived from embryonic precursors seeded during fetal development[42,154,170]. Though few in number, Ly6C^{+} monocytes constitutively enter the peritoneal cavity in a CCR2-dependent manner and act as precursors of LPMs[171]. We have demonstrated that Msln/Muc16 interact with LPMs along their differentiation axis to promote TRM identity. However, the timing of this interaction along the developmental trajectory of macrophages and the organism remains unknown. Additionally, whether the cells interacting with

Msln/Muc16 are in the fluid phase or are adherent to the mesothelium is also unclear. We examined the capability of peritoneal fluid to induce Gata6 in monocytes and did not detect significant upregulation (data not shown). At the steady state in adult mice, while a majority are embryonically derived, a small proportion come from the periphery as monocytes[154]. In young mice, however, almost all LPMs are embryo-derived[44,172] and do not experience a monocyte stage. We hypothesize that this potentially explains why we do not detect a difference in Gata6 expression in young mice and why the effect becomes more significant when original LPMs are replenished by peripheral monocytes in the settings of aging, irradiation, and inflammation-induced cell death. While we have identified the importance of Msln and Muc16, the role of other factors from the local peritoneal environment in defining the identity of TRM remains to be studied.

Msln was first studied as a pro-tumorigenic protein and used as a tumor biomarker. However, the roles of Msln in other cell types were not well studied[108]. During homeostasis, expression of Msln is limited to cavities derived from the intraembryonic coelom which may explain the localized effect of knocking out Msln and Muc16 at steady state. In contrast to its effect on macrophages, the loss of Msln seems to have limited effects on mesothelium at the level of proliferation, cytokine secretion, and adhesion (data not shown). Prior to our study, peritoneal mesothelium was known to produce M-CSF and other growth factors to support TRM differentiation[144]. Beyond the role as an adhesion protein[173,174], Msln affected macrophage adhesion, migration, and other macrophage biology and did not find any difference (data not shown). It was previously reported that Gata6 controls the survival of LPM[134,135]. However, we did not observe any defect in proliferation and survival in LPMs from mice lacking Msln/Muc16, even though they shared several features with *Gata6*$^{f/f}$, LysM-Cre mice. We observed fewer Gata6+ LPMs in mice lacking Msln/Muc16, but the

lower magnitude of the effect may explain why *Msln*$^{-/-}$ and *Muc16*$^{-/-}$ mice do not recapitulate every phenotype in *Gata6*$^{f/f}$, LysM-Cre mice, including cell number and certain surface markers[40,134,135]. Given that the difference in Gata6+ LPM was greater in mice challenged with different model injuries, we hypothesis that Msln and Muc16 may play an even more important role outside of homeostasis that is yet unrecognized.

In the zymosan-induced peritonitis model, we found more neutrophils infiltrated into the peritoneal cavity in the acute phase[46] and less mature macrophages were present in the resolution phase in both *Msln*$^{-/-}$ and *Muc16*$^{-/-}$ animals. However, it is still not clear whether this is due to mesothelial or myeloid cells, as Msln blockade in surgery-induced peritoneal adhesions[109] eliminated adhesion. Regardless, the interaction between mesothelial cells and LPMs[175] and the role of peritoneal macrophages in peritoneal dialysis patients[176] suggests that Msln could be a potential therapeutic target. Future studies of Msln should clarify its biochemical interactions with Muc16 and potential receptors, illuminate its role in modulating Gata6 and tissue-specific transcription factors, and determine its importance outside of homeostasis.

CHAPTER THREE

Msln orchestrates mucosal repair and tumorigenesis in a macrophage-dependent manner

Chapter 3: Abstract
Msln is expressed in many different carcinomas, however little is known about the function and influence of Msln in immune cells residing in the tumors. We found that Msln was one of the most upregulated genes in epithelial cells after colonic biopsy injury. To determine whether Msln had a function in this model, we injured WT and Msln-deficient mice. We found that Msln-deficient mice had more proinflammatory cells in the wound bed. We next hypothesized that Msln had a similar role in modulating immune cells in $APC^{Min/+}$ mice to allow for larger polyp growth. We found that Msln-deficient $APC^{Min/+}$ mice had on average smaller polyps and the maximum diameter of polyp in each mouse was smaller than in WT $APC^{Min/+}$ mice. These results suggest that epithelial-derived Msln may be functioning to promote a pro-regenerative, pro-tumor microenvironment by immunosuppression.

Chapter 3: Introduction

Msln is expressed in many cancers including intestinal cancers in humans[177], though its role in promoting intestinal cancer is unknown. One model of intestinal cancer is the $APC^{min/+}$ mouse model of intestinal polyposis[178]. In this mouse model, one allele of adenomatous polyposis coli (APC) is mutated and polyps start to form throughout the small and large intestine over time by loss of heterozygosity. The majority of the polyps form throughout the small intestine and several polyps typically form in the colon. Loss of APC leads to stabilization of β-catenin and activation of the Wnt signaling pathway.

We were interested in the role of Msln because we found that it was one of the most upregulated genes in WAE cells compared to uninjured epithelial cells after biopsy injury. Due to its purported role in adhesion, proliferation, and cancer, we hypothesized that Msln would be important for proper healing after intestinal epithelial injury. We made Msln conditioned knockout mice and injured these mice to look for intestinal healing defects. Surprisingly, the major defects we found were in the mesenchyme within the wound bed once the epithelium-derived Msln was depleted. There were more Ly6G+ neutrophils within the wound beds compared to WT mice. These results suggested that Msln was important for controlling inflammation after intestinal mucosal injury. We also crossed $Msln^{-/-}$ mice with $APC^{min/+}$ mice to examine the role of Msln in intestinal cancer formation and growth. We found that $Msln^{-/-}$ mice had smaller polyps in the small intestine compared to $Msln^{+/+}$ mice in this model. These results suggest that Msln may be important for recruiting and/or maintaining the tumor microenvironment in mesothelin-expressing carcinomas.

Chapter 3: Methods and Materials

Mice

Animal experiments were performed in accordance with approved protocols from the Washington University School of Medicine Animal Studies Committee. *APC*$^{min/+}$ mice were obtained from Jackson labs and were bred to generate *APC*$^{min/+}$ mice that were WT, heterozygous, or knockout for *Msln*.

Polyinosinic-polycytidylic acid [poly(I:C)] injury

Blunted villi were induced by intraperitoneal injection of Poly(I:C) (Sigma) 0.5mg/25g mouse.

Colonic biopsy

We used a high-resolution miniaturized colonoscope system to visualize the lumen of the colon and discretely injure the mucosal layer in 10-16 week old anesthetized mice. After inflating the colon with PBS, we inserted 3 French flexible biopsy forceps into the sheath adjacent to the camera. We removed 3-5 full-thickness areas of the entire mucosa and submucosa that were distributed along the dorsal side of the colon. All mice were injured with the same technique. For this study, we evaluated wounds that averaged ~1 mm2, which is equivalent to removal of ~300 crypts.

Colonic tissue preparation

For fixed-frozen sections, wounded mice were sacrificed and perfused transcardially with 4% paraformaldehyde (PFA). After dissection, the colon was inflated with 4% PFA, opened longitudinally, and pinned flat in 4% PFA overnight. The following day the fixed colons were

incubated in 20% sucrose-PBS for 6 hours. For frozen sections, colons were removed, washed in PBS, and placed in OCT compound (Tissue-Tek).

For both procedures, each wound bed, including 1-2 mm of adjacent uninjured area, was removed with a razor blade and frozen in OCT compound. For each individual wound, the material was oriented so that serial 5-µm-thick sections were obtained in a proximal to distal manner with respect to the orientation of the *in vivo* colon. Each wound bed was completely sectioned. To standardize our analysis, we evaluated the 5-10 sections in the central (largest) portion of a given wound bed as determined by light microscopic views of unstained sections. Serially numbered, unstained sections were stored at -80°C until use. One of these sections was stained with hematoxylin/eosin to confirm orientation.

In situ hybridization

Tissues were fixed in 4% (v/v) paraformaldehyde at 4ºC for 18 to 24 hours, dehydrated with 20% sucrose in PBS, and embedded in OCT. Tissue sections cut at a thickness of 5 µm were processed for RNA in situ detection using the RNAscope 2.5 HD Assay–RED according to the manufacturer's instructions (Advanced Cell Diagnostics). RNAscope probes used were Mm-MSLN (Cat No. 443241).

Immunofluorescence

Fresh-frozen sections of wounds were used for immunofluorescence. Sections were fixed in 4% PFA, rinsed in PBS, blocked in 3% BSA/0.1% Triton-X for 20 minutes and incubated with primary antibody for one hour. Slides were then rinsed with PBS, incubated with secondary antibody

followed by bis-benzimide staining and mounting with Mowiol 4-88 (Calbiochem). Sections were viewed with a Zeiss Axiovert 200 with Axiocam MRM camera. Antibodies used were rat monoclonal anti-CD31 (MEC 13.3; BD Biosciences), rat monoclonal anti-KI67 (TEC-3; DAKO), monoclonal rat anti-F4/80 (CI:A3-1;Caltag Laboratories), and rabbit polyclonal anti-β-catenin (Sigma). All primary antibodies were used at 1:100 dilution. Appropriate donkey anti-rat or anti-rabbit secondary antibodies conjugated to Alexa Fluor 488 or Alexa Fluor 594 (Invitrogen) were used at 1:500 dilution to visualize staining.

Quantification of polyps from APC$^{min/+}$ mice.

Mice were sacrificed at four months of age, the small intestine was removed and flushed with PBS, and the small intestine was inflated with 4% PFA for 30 seconds. The small intestine was then opened longitudinally and pinned open in 4% PFA and fixed overnight at 4°C. The intestine was then examined under a stereoscope and each polyp was photographed (Olympus, Tokyo, Japan). The size and number of each polyp was recorded for each mouse.

Chapter 3: Results

We started our investigation on Msln first because it was one of the most highly upregulated genes in wound-associated epithelial cells compared to uninjured epithelial cells upon biopsy injury. To confirm that Msln was expressed specifically in epithelial cells, we performed in situ hybridization on WT wounds four days after injury (**Figure 3.1.A**). We found that Msln was only expressed in WAE cells and was not expressed in any mesenchymal cells. We have also utilized a well-characterized poly(I:C)-mediated injury model, known to selectively ablate the small intestinal villus epithelium with sparing of crypts and showed that Msln was expressed in the WAE cells

(**Figure 3.1.B**). As a positive control, Msln expression could be observed in mesothelial cells lining the outer layer of the intestine.

To study the role of Msln in wound-associated epithelial cells, we obtained and injured VilCre X $Msln^{f/f}$ and $Msln^{f/f}$ mice. We found that injured VilCre X $Msln^{f/f}$ mice had more Ly6G+ neutrophils 4 days after biopsy injury (**Figure 3.2**). However, the wound healed comparably between VilCre X $Msln^{f/f}$ and $Msln^{f/f}$ mice by day 12. Taken together, these results suggest that Msln has an anti-inflammatory role on promoting wound repair.

We next wanted to determine the role of Msln in promoting intestinal polyp formation in the $APC^{Min/+}$ model. We crossed $APC^{Min/+}$ mice with $Msln^{+/-}$ mice to generate $APC^{Min/+}$ mice that were wildtype (WT), heterozygous (Het), or knockout (KO) for the *Msln* gene. We sacrificed mice at four months of age and counted and measured the size of all polyps in the small intestine. We found that $Msln^{-/-}$ mice had fewer large polyps (>2 mm diameter) and the largest polyp (maximum diameter) was smaller compared to WT mice (**Figure 3.3**). These results suggest that Msln is required for maximal polyp growth in the $APC^{min/+}$ model of intestinal polyposis.

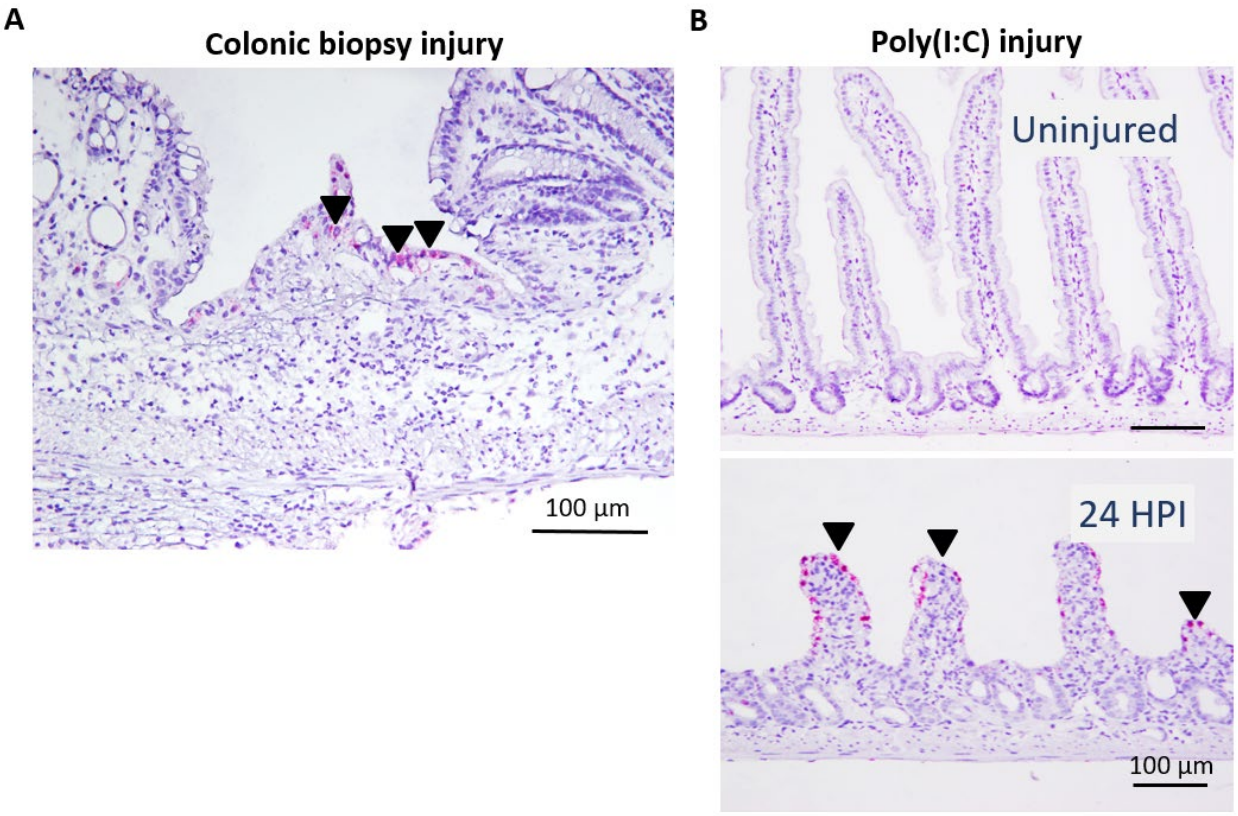

Figure 3.1. *Msln* expression in the wound

(A) Representative RNA scope images for Msln in fresh-frozen intestine section. Black arrowheads indicate Msln-positive wound-associated epithelial cells Poly(I:C) 24 hr post ip.

(B) Representative RNA scope images for Msln in fresh-frozen intestine section. Black arrowheads indicate Msln-positive wound-associated epithelial cells 4 day post biopsy.

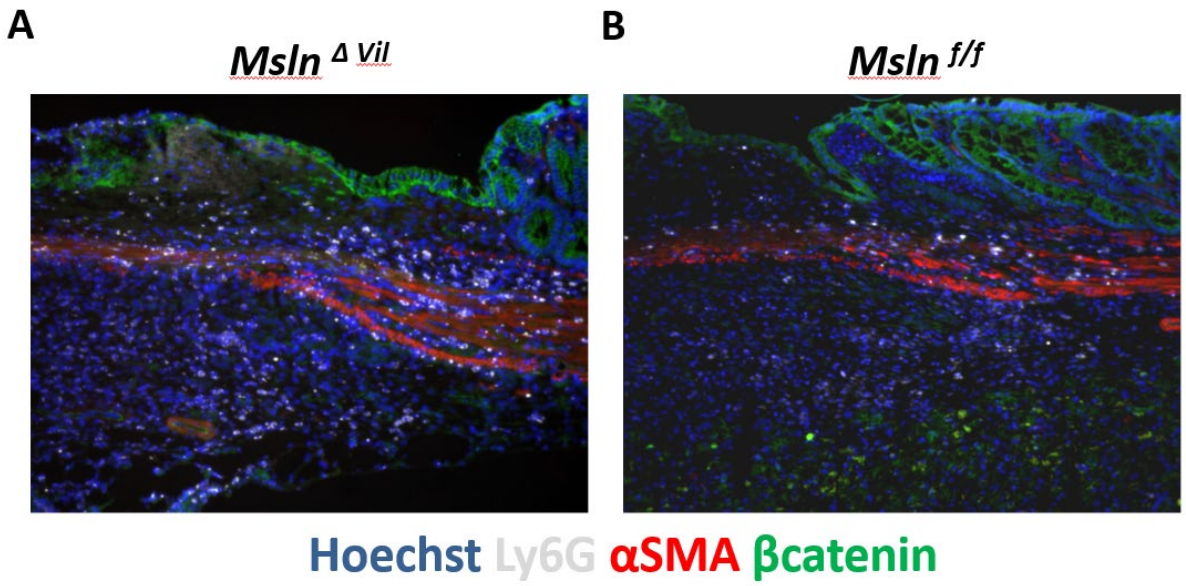

Figure 3.2. More Ly6G+ neutrophils accumulate in the wound bed in Msln-deficient mice

Sections of colons from (A) VilCre X *Msln*$^{f/f}$ and (B) *Msln*$^{f/f}$ mice 3 days post-biopsy. The sections were stained with anti-Ly6G (grey) to detect neutrophils, anti-α-SMA antisera (red) to detect muscularis propria, anti-β-catenin (green) to detect the epithelium, and bis-benzamide to label nuclei (blue).

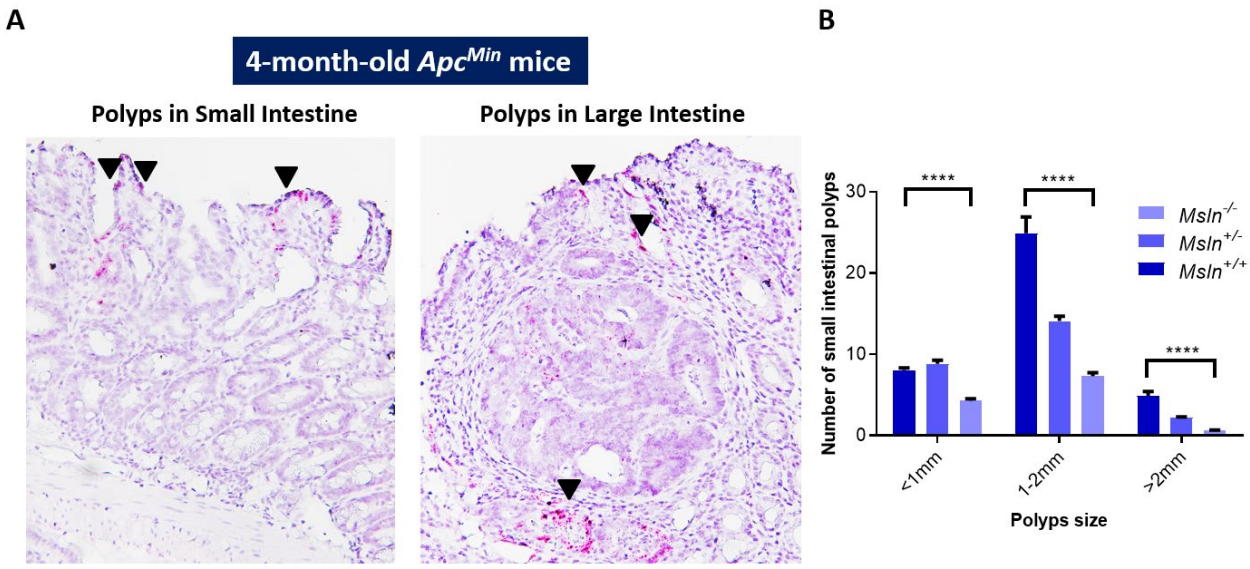

Fig 3 *Msln* expression in the WAE-like cell and the impact on the number of polyps

(A) Representative RNA scope images for Msln in fresh-frozen intestine section. Black arrowheads indicate Msln-positive WAE-like cells **(B)** Graph of the average number of small intestinal polyps less than 1 mm, 1-2 mm, and greater than 2 mm in $Apc^{Min/+}$ mice sacrificed at 4 months of age. *n*=13 WT, *n*=20 Het, *n*=17 KO mice. ANOVAs were run between WT, Het, and KO for each category of size of polyps and only polyps greater than 2 mm had a significant difference. ****P<0.0001 by Tukey's post-test.

Chapter 3: Discussion

We showed the impact of Msln on tissue resident macrophage differentiation in the peritoneum. In other microenvironments, e.g. epithelium, Msln may also modulate the differentiation of infiltrated monocytes. Msln is known to be expressed by intestinal epithelium in a YAP dependent manner during *Apc* mutant aberrant crypt foci[179] and by wound associated epithelial-like cells in our *in vitro* primary epithelial cell culture system[180]. We hypothesized that understanding the role of Msln in colonic wound repair would also shed light on the role of Msln during cancer. Our data would suggest that this may interact with tissue-resident or infiltrating myeloid cells and modulate their function. Tumors have been described as wounds that do not heal because many of the processes required for wound repair are also required for tumor growth[181]. In $APC^{Min/+}$ mice, there was no significant difference in the number of small or medium sized polyps, suggesting that Msln is not required for the initiation of polyps but instead is important for their growth above 2 mm. Although speculative, our work would indicate that Msln may function in cancer to adjust the tumor microenvironment to produce a M2-skewed macrophage phenotype which is beneficial to the tumorigenesis.

Msln was originally discovered as a cytokine that could act similarly to IL-6 in a megakaryocyte colony-forming assay[149], though the majority of the recent research on this gene has been investigating its role as a membrane protein expressed on cancer cells[182]. It is also utilized as a target for antibody-based cancer immunotherapies. Our results suggest that Msln may be acting as a cytokine in our wound healing and tumorigenesis model because the major defects were seen in cell types that do not express Msln. Future studies should determine which portions of Msln were required for granulation tissue formation (MPF, mature Msln, or both);

which cell type(s) are influenced by the different microenvironments. Additionally, direct blockade of Msln using neutralizing antibodies may be an attractive therapeutic approach for Msln-expressing cancers, since Msln is not thought to have any role under homeostatic conditions[88].

CHAPTER FOUR

Summary and Future Directions

Summary

As a heterogeneous population of immune cells, TRMs fulfill tissue-specific and niche-specific functions. These cover from well-regulated homeostatic functions to central roles in tissue immune surveillance, response to infection and the resolution of inflammation. Recent studies highlight marked differences in the origins of tissue macrophages that arise from hematopoietic versus self-renewing embryo-derived populations. Understanding the mechanisms that dictate TRM heterogeneity should explain why conventional models of macrophage activation, i.e. BMDM, do not interconvert the extent of heterogeneity seen *in vivo*.

In addition to delineating transcriptional modulation within tissue resident macrophages, we provide new insights about the role of niche factors in shaping the identity of these unique cells. Dietary derived retinoic acid induces LPM-specific TF Gata6 expression. We hypothesized that microenvironment also imprints the TRMs because of proximity. We accessed the effect of soluble proteins from mesothelium-lining serous cavities on Gata6 regulation. We next did informatics analysis to identify potent candidates. We also applied both BM chimera and adoptive transfer approaches to validate if the mechanism of Msln/Muc16-mediated Gata6 regulation acts extrinsically. We found that mesothelial derived Msln and Muc16 induce Gata6 expression at both steady state and inflammation, which further influence the immune responses to sterile inflammation and pathogen infection. Targeting both ligands may provide a new therapeutic approach for macrophage-related diseases.

On the other side, there are many macrophage-related intestinal diseases that are characterized by inflammation and loss of crypts, though the mechanisms by which the mucosa regenerates after

injury are unclear. We utilized a colonic biopsy injury system to create focal wounds in the distal colon of mice to study the mechanisms of mucosal repair. We hypothesized that understanding mucosal repair would provide insight into the mechanisms of intestinal diseases that involve loss of crypts and/or incomplete healing such as IBD.

We evaluated epithelial-derived genes stimulated after injury and surprisely found that Msln was upregulated during inflammation. We found that Msln-deficient mice had more proinflammatory cells in the wound bed. Also, Msln-deficient $APC^{Min/+}$ mice had smaller polyps in the small intestine than $APC^{Min/+}$ mice. It suggests that Msln is an epithelial-derived factor that is required to stimulate tissue repair after epithelial injury or carcinoma.

The findings described in this thesis suggest that tissue-specific factors are critical for TRM differentiation and colon regeneration after mucosal damage. These results may eventually lead to therapies that establishing macrophages for repair (locally-injected recombinant Msln) or inhibit pro-tumorigenesis to limit tumor growth (anti-Msln therapy).

Future directions

Msln and Mucin16 as targets for tissue immunity

We found that mesothelial cell-derived Msln and Muc16 imprint Gata6-positive TRMs and WAE cell-derived Msln modulates the microenvironment in the wound bed. But the signaling pathways for both phenomena are still unknown. Given that Gata6 defect results in abnormal immune responses during inflammation, we presumed that both proteins immune-modulate the TRMs to resolve the inflammation properly. We are continuing to generate recombinant Msln and MPF to rescue the defect we found in mice lack of Msln and Muc16.

The other direction is to find the receptor for both Msln and Muc16. The receptor and signaling mechanism in LPMs that leads to the effect of Msln and Muc16 on Gata6 expression remains to be identified. By literature research, we found two candidates, Mrc1 and Siglece, which interact with either Msln or Muc16. We found that both WT and *Mrc1*$^{-/-}$ CD45.2 BM-derived cells colonized the peritoneum and pleura of WT CD45.1 recipient mice to produce comparable number of Gata6+ tissue resident macrophages in the peritoneum and lung pleura. After adoptively transferring either CD45.2 WT or *Mrc1*$^{-/-}$ monocytes and BMDMs, donor-derived LPMs has similar F4/80 and Gata6 expression in the WT recipient mice. To examine the other target, we are planning to get Siglece reagents.

The other part is to figure out which portions of Msln have the bioactivity in modulating Gata6 expression in tissue resident macrophages. We are currently generating MPF, mature Msln, or full-length non-cleavable forms of Msln so that we can purify the proteins and test their ability to

directly stimulate pre-macrophages such as monocytes and BMDMs. These experiments should provide some clues as to which portions of Msln are responsible for LPM differentiation.

We hypothesize that there is a common mechanism for the accumulated pro-inflammatory cells seen in colonic wounds and the smaller polyps seen in $APC^{Min/+}$ mice. Msln expression is associated with a worse prognosis in cancer patients and Msln is commonly thought to function as a cell-intrinsic tumor-promoter[182]. Although Msln expression appears to be important for cell-intrinsic effects in cancer, our wounding experiments suggest that Msln may have an effect on a broader range of cell types than previously appreciated. Our hypothesis is that Msln has anti-inflammatory capability and its expression in carcinomas is important for recruitment and/or establishment of the tumor microenvironment. Macrophages are one of the major cell types that are recruited to both colonic wounds and tumors. Tumor associated macrophages are required for tumor growth and may explain why polyps were smaller in $Msln^{-/-};APC^{Min/+}$ mice compared to WT;$APC^{Min/+}$ mice. Future studies should investigate whether there are reduced macrophages in $Msln^{-/-}$ polyps, and whether blocking Msln may be an effective approach to treating Msln-positive tumors.

References

1. Cavaillon, J.M. The historical milestones in the understanding of leukocyte biology initiated by Elie Metchnikoff. *J Leukoc Biol* **90**, 413-424 (2011).

2. Gordon, S. & Taylor, P.R. Monocyte and macrophage heterogeneity. *Nat Rev Immunol* **5**, 953-964 (2005).

3. Wynn, T.A., Chawla, A. & Pollard, J.W. Macrophage biology in development, homeostasis and disease. *Nature* **496**, 445-455 (2013).

4. Sherr, C.J. The colony-stimulating factor 1 receptor: pleiotropy of signal-response coupling. *Lymphokine Res* **9**, 543-548 (1990).

5. Ginhoux, F. & Guilliams, M. Tissue-Resident Macrophage Ontogeny and Homeostasis. *Immunity* **44**, 439-449 (2016).

6. Hoeffel, G. & Ginhoux, F. Ontogeny of Tissue-Resident Macrophages. *Front Immunol* **6**, 486 (2015).

7. Murray, P.J. & Wynn, T.A. Protective and pathogenic functions of macrophage subsets. *Nat Rev Immunol* **11**, 723-737 (2011).

8. Guilliams, M.*, et al.* Unsupervised High-Dimensional Analysis Aligns Dendritic Cells across Tissues and Species. *Immunity* **45**, 669-684 (2016).

9. Tamoutounour, S.*, et al.* CD64 distinguishes macrophages from dendritic cells in the gut and reveals the Th1-inducing role of mesenteric lymph node macrophages during colitis. *Eur J Immunol* **42**, 3150-3166 (2012).

10. Tamoutounour, S.*, et al.* Origins and functional specialization of macrophages and of conventional and monocyte-derived dendritic cells in mouse skin. *Immunity* **39**, 925-938 (2013).

11. Nakajima, K. & Kohsaka, S. Functional roles of microglia in the brain. *Neurosci Res* **17**, 187-203 (1993).

12. Trapnell, B.C., Whitsett, J.A. & Nakata, K. Pulmonary alveolar proteinosis. *N Engl J Med* **349**, 2527-2539 (2003).

13. Zhang, D.E., Hetherington, C.J., Chen, H.M. & Tenen, D.G. The macrophage transcription factor PU.1 directs tissue-specific expression of the macrophage colony-stimulating factor receptor. *Mol Cell Biol* **14**, 373-381 (1994).

14. DeKoter, R.P. & Singh, H. Regulation of B lymphocyte and macrophage development by graded expression of PU.1. *Science* **288**, 1439-1441 (2000).

15. Pham, T.H.*, et al.* Mechanisms of in vivo binding site selection of the hematopoietic master transcription factor PU.1. *Nucleic Acids Res* **41**, 6391-6402 (2013).

16. Wang, Y.*, et al.* IL-34 is a tissue-restricted ligand of CSF1R required for the development of Langerhans cells and microglia. *Nat Immunol* **13**, 753-760 (2012).

17. Greter, M.*, et al.* Stroma-derived interleukin-34 controls the development and maintenance of langerhans cells and the maintenance of microglia. *Immunity* **37**, 1050-1060 (2012).

18. Ginhoux, F.*, et al.* Fate mapping analysis reveals that adult microglia derive from primitive macrophages. *Science* **330**, 841-845 (2010).

19. Behre, G.*, et al.* c-Jun is a JNK-independent coactivator of the PU.1 transcription factor. *J Biol Chem* **274**, 4939-4946 (1999).

20. Aziz, A., Soucie, E., Sarrazin, S. & Sieweke, M.H. MafB/c-Maf deficiency enables self-renewal of differentiated functional macrophages. *Science* **326**, 867-871 (2009).

21. Soucie, E.L.*, et al.* Lineage-specific enhancers activate self-renewal genes in macrophages and embryonic stem cells. *Science* **351**, aad5510 (2016).

22. Brockes, J.P. & Kumar, A. Appendage regeneration in adult vertebrates and implications for regenerative medicine. *Science* **310**, 1919-1923 (2005).

23. Moriguchi, T.*, et al.* MafB is essential for renal development and F4/80 expression in macrophages. *Mol Cell Biol* **26**, 5715-5727 (2006).

24. Aziz, A.*, et al.* Development of macrophages with altered actin organization in the absence of MafB. *Mol Cell Biol* **26**, 6808-6818 (2006).

25. Mass, E.*, et al.* Specification of tissue-resident macrophages during organogenesis. *Science* **353**(2016).

26. Geissmann, F.*, et al.* Development of monocytes, macrophages, and dendritic cells. *Science* **327**, 656-661 (2010).

27. Gautier, E.L.*, et al.* Gene-expression profiles and transcriptional regulatory pathways that underlie the identity and diversity of mouse tissue macrophages. *Nat Immunol* **13**, 1118-1128 (2012).

28. Guilliams, M. & Scott, C.L. Does niche competition determine the origin of tissue-resident macrophages? *Nat Rev Immunol* **17**, 451-460 (2017).

29. Lavin, Y., Mortha, A., Rahman, A. & Merad, M. Regulation of macrophage development and function in peripheral tissues. *Nat Rev Immunol* **15**, 731-744 (2015).

30. Ghosn, E.E.*, et al.* Two physically, functionally, and developmentally distinct peritoneal macrophage subsets. *Proc Natl Acad Sci U S A* **107**, 2568-2573 (2010).

31. Austyn, J.M. & Gordon, S. F4/80, a monoclonal antibody directed specifically against the mouse macrophage. *Eur J Immunol* **11**, 805-815 (1981).

32. Taylor, P.R.*, et al.* Macrophage receptors and immune recognition. *Annu Rev Immunol* **23**, 901-944 (2005).

33. Taylor, P.R., Brown, G.D., Geldhof, A.B., Martinez-Pomares, L. & Gordon, S. Pattern recognition receptors and differentiation antigens define murine myeloid cell heterogeneity ex vivo. *Eur J Immunol* **33**, 2090-2097 (2003).

34. Hickstein, D.D.*, et al.* Isolation and characterization of the receptor on human neutrophils that mediates cellular adherence. *J Biol Chem* **262**, 5576-5580 (1987).

35. Shortman, K. & Liu, Y.J. Mouse and human dendritic cell subtypes. *Nat Rev Immunol* **2**, 151-161 (2002).

36. Kantor, A.B., Stall, A.M., Adams, S., Herzenberg, L.A. & Herzenberg, L.A. Differential development of progenitor activity for three B-cell lineages. *Proc Natl Acad Sci U S A* **89**, 3320-3324 (1992).

37. Ghosn, E.E., Yang, Y., Tung, J., Herzenberg, L.A. & Herzenberg, L.A. CD11b expression distinguishes sequential stages of peritoneal B-1 development. *Proc Natl Acad Sci U S A* **105**, 5195-5200 (2008).

38. Casasnovas, J.M., Springer, T.A., Liu, J.H., Harrison, S.C. & Wang, J.H. Crystal structure of ICAM-2 reveals a distinctive integrin recognition surface. *Nature* **387**, 312-315 (1997).

39. de Fougerolles, A.R., Stacker, S.A., Schwarting, R. & Springer, T.A. Characterization of ICAM-2 and evidence for a third counter-receptor for LFA-1. *J Exp Med* **174**, 253-267 (1991).

40. Okabe, Y. & Medzhitov, R. Tissue-specific signals control reversible program of localization and functional polarization of macrophages. *Cell* **157**, 832-844 (2014).

41. Uderhardt, S.*, et al.* 12/15-lipoxygenase orchestrates the clearance of apoptotic cells and maintains immunologic tolerance. *Immunity* **36**, 834-846 (2012).

42. Yona, S.*, et al.* Fate mapping reveals origins and dynamics of monocytes and tissue macrophages under homeostasis. *Immunity* **38**, 79-91 (2013).

43. Cain, D.W.*, et al.* Identification of a tissue-specific, C/EBPbeta-dependent pathway of differentiation for murine peritoneal macrophages. *J Immunol* **191**, 4665-4675 (2013).

44. Schulz, C.*, et al.* A lineage of myeloid cells independent of Myb and hematopoietic stem cells. *Science* **336**, 86-90 (2012).

45. Kim, K.W.*, et al.* MHC II+ resident peritoneal and pleural macrophages rely on IRF4 for development from circulating monocytes. *J Exp Med* **213**, 1951-1959 (2016).

46. Davies, L.C.*, et al.* Distinct bone marrow-derived and tissue-resident macrophage lineages proliferate at key stages during inflammation. *Nat Commun* **4**, 1886 (2013).

47. Bujko, A.*, et al.* Transcriptional and functional profiling defines human small intestinal macrophage subsets. *J Exp Med* **215**, 441-458 (2018).

48. Bain, C.C.*, et al.* Resident and pro-inflammatory macrophages in the colon represent alternative context-dependent fates of the same Ly6Chi monocyte precursors. *Mucosal Immunol* **6**, 498-510 (2013).

49. Bernardo, D.*, et al.* Human intestinal pro-inflammatory CD11c(high)CCR2(+)CX3CR1(+) macrophages, but not their tolerogenic CD11c(-)CCR2(-)CX3CR1(-) counterparts, are expanded in inflammatory bowel disease. *Mucosal Immunol* **11**, 1114-1126 (2018).

50. Rugtveit, J.*, et al.* Cytokine profiles differ in newly recruited and resident subsets of mucosal macrophages from inflammatory bowel disease. *Gastroenterology* **112**, 1493-1505 (1997).

51. Mahida, Y.R., Wu, K.C. & Jewell, D.P. Respiratory burst activity of intestinal macrophages in normal and inflammatory bowel disease. *Gut* **30**, 1362-1370 (1989).

52. Schridde, A.*, et al.* Tissue-specific differentiation of colonic macrophages requires TGFbeta receptor-mediated signaling. *Mucosal Immunol* **10**, 1387-1399 (2017).

53. Kumawat, A.K.*, et al.* Expression and characterization of alphavbeta5 integrin on intestinal macrophages. *Eur J Immunol* **48**, 1181-1187 (2018).

54. Henson, P.M. Cell Removal: Efferocytosis. *Annu Rev Cell Dev Biol* **33**, 127-144 (2017).

55. Lacy-Hulbert, A.*, et al.* Ulcerative colitis and autoimmunity induced by loss of myeloid alphav integrins. *Proc Natl Acad Sci U S A* **104**, 15823-15828 (2007).

56. Niess, J.H.*, et al.* CX3CR1-mediated dendritic cell access to the intestinal lumen and bacterial clearance. *Science* **307**, 254-258 (2005).

57. Kim, K.W.*, et al.* In vivo structure/function and expression analysis of the CX3C chemokine fractalkine. *Blood* **118**, e156-167 (2011).

58. Shaw, T.N.*, et al.* Tissue-resident macrophages in the intestine are long lived and defined by Tim-4 and CD4 expression. *J Exp Med* **215**, 1507-1518 (2018).

59. Fadok, V.A.*, et al.* Macrophages that have ingested apoptotic cells in vitro inhibit proinflammatory cytokine production through autocrine/paracrine mechanisms involving TGF-beta, PGE2, and PAF. *J Clin Invest* **101**, 890-898 (1998).

60. Kelly, A.*, et al.* Human monocytes and macrophages regulate immune tolerance via integrin alphavbeta8-mediated TGFbeta activation. *J Exp Med* **215**, 2725-2736 (2018).

61. Grimm, M.C.*, et al.* Direct evidence of monocyte recruitment to inflammatory bowel disease mucosa. *J Gastroenterol Hepatol* **10**, 387-395 (1995).

62. Kamada, N.*, et al.* Unique CD14 intestinal macrophages contribute to the pathogenesis of Crohn disease via IL-23/IFN-gamma axis. *J Clin Invest* **118**, 2269-2280 (2008).

63. Thiesen, S.*, et al.* CD14(hi)HLA-DR(dim) macrophages, with a resemblance to classical blood monocytes, dominate inflamed mucosa in Crohn's disease. *J Leukoc Biol* **95**, 531-541 (2014).

64. Mahida, Y.R., Patel, S., Gionchetti, P., Vaux, D. & Jewell, D.P. Macrophage subpopulations in lamina propria of normal and inflamed colon and terminal ileum. *Gut* **30**, 826-834 (1989).

65. Schenk, M., Bouchon, A., Seibold, F. & Mueller, C. TREM-1--expressing intestinal macrophages crucially amplify chronic inflammation in experimental colitis and inflammatory bowel diseases. *J Clin Invest* **117**, 3097-3106 (2007).

66. Vos, A.C.*, et al.* Regulatory macrophages induced by infliximab are involved in healing in vivo and in vitro. *Inflamm Bowel Dis* **18**, 401-408 (2012).

67. Laverriere, A.C.*, et al.* GATA-4/5/6, a subfamily of three transcription factors transcribed in developing heart and gut. *J Biol Chem* **269**, 23177-23184 (1994).

68. Jiang, Y. & Evans, T. The Xenopus GATA-4/5/6 genes are associated with cardiac specification and can regulate cardiac-specific transcription during embryogenesis. *Dev Biol* **174**, 258-270 (1996).

69. Gove, C.*, et al.* Over-expression of GATA-6 in Xenopus embryos blocks differentiation of heart precursors. *EMBO J* **16**, 355-368 (1997).

70. Michailova, K.N. & Usunoff, K.G. Serosal membranes (pleura, pericardium, peritoneum). Normal structure, development and experimental pathology. *Adv Anat Embryol Cell Biol* **183**, i-vii, 1-144, back cover (2006).

71. Gaudio, E., Rendina, E.A., Pannarale, L., Ricci, C. & Marinozzi, G. Surface morphology of the human pleura. A scanning electron microscopic study. *Chest* **93**, 149-153 (1988).

72. Chan, R.*, et al.* Characterization of two monoclonal antibodies in an immunohistochemical study of keratin 8 and 18 expression. *Am J Clin Pathol* **89**, 472-480 (1988).

73. Zhu, Z., Yao, J., Wang, F. & Xu, Q. TNF-alpha and the phenotypic transformation of human peritoneal mesothelial cell. *Chin Med J (Engl)* **115**, 513-517 (2002).

74. Breborowicz, A., Wieczorowska, K., Martis, L. & Oreopoulos, D.G. Glycosaminoglycan chondroitin sulphate prevents loss of ultrafiltration during peritoneal dialysis in rats. *Nephron* **67**, 346-350 (1994).

75. Breborowicz, A.*, et al.* The effect of N-acetylglucosamine as a substrate for in vitro synthesis of glycosaminoglycans by human peritoneal mesothelial cells and fibroblasts. *Adv Perit Dial* **14**, 31-35 (1998).

76. Yung, S. & Chan, T.M. Mesothelial cells. *Perit Dial Int* **27 Suppl 2**, S110-115 (2007).

77. Cheong, Y.C.*, et al.* Peritoneal healing and adhesion formation/reformation. *Hum Reprod Update* **7**, 556-566 (2001).

78. Yung, S. & Chan, T.M. Pathophysiological changes to the peritoneal membrane during PD-related peritonitis: the role of mesothelial cells. *Mediators Inflamm* **2012**, 484167 (2012).

79. diZerega, G.S. & Campeau, J.D. Peritoneal repair and post-surgical adhesion formation. *Hum Reprod Update* **7**, 547-555 (2001).

80. Elmadbouh, I.*, et al.* Mesothelial cell transplantation in the infarct scar induces neovascularization and improves heart function. *Cardiovasc Res* **68**, 307-317 (2005).

81. Meier, S. Development of the chick embryo mesoblast: pronephros, lateral plate, and early vasculature. *J Embryol Exp Morphol* **55**, 291-306 (1980).

82. Yamaguchi, N.*, et al.* A novel cytokine exhibiting megakaryocyte potentiating activity from a human pancreatic tumor cell line HPC-Y5. *J Biol Chem* **269**, 805-808 (1994).

83. Chang, K. & Pastan, I. Molecular cloning of mesothelin, a differentiation antigen present on mesothelium, mesotheliomas, and ovarian cancers. *Proc Natl Acad Sci U S A* **93**, 136-140 (1996).

84. Zhang, Y., Chertov, O., Zhang, J., Hassan, R. & Pastan, I. Cytotoxic activity of immunotoxin SS1P is modulated by TACE-dependent mesothelin shedding. *Cancer Res* **71**, 5915-5922 (2011).

85. Zwaenepoel, I.*, et al.* Otoancorin, an inner ear protein restricted to the interface between the apical surface of sensory epithelia and their overlying acellular gels, is defective in autosomal recessive deafness DFNB22. *Proc Natl Acad Sci U S A* **99**, 6240-6245 (2002).

86. Sathyanarayana, B.K., Hahn, Y., Patankar, M.S., Pastan, I. & Lee, B. Mesothelin, Stereocilin, and Otoancorin are predicted to have superhelical structures with ARM-type repeats. *BMC Struct Biol* **9**, 1 (2009).

87. Ma, J., Tang, W.K., Esser, L., Pastan, I. & Xia, D. Characterization of crystals of an antibody-recognition fragment of the cancer differentiation antigen mesothelin in complex with the therapeutic antibody MORAb-009. *Acta Crystallogr Sect F Struct Biol Cryst Commun* **68**, 950-953 (2012).

88. Bera, T.K. & Pastan, I. Mesothelin is not required for normal mouse development or reproduction. *Mol Cell Biol* **20**, 2902-2906 (2000).

89. Sato, N.*, et al.* Frequent hypomethylation of multiple genes overexpressed in pancreatic ductal adenocarcinoma. *Cancer Res* **63**, 4158-4166 (2003).

90. Chen, S.H., Hung, W.C., Wang, P., Paul, C. & Konstantopoulos, K. Mesothelin binding to CA125/MUC16 promotes pancreatic cancer cell motility and invasion via MMP-7 activation. *Sci Rep* **3**, 1870 (2013).

91. Yen, M.J.*, et al.* Diffuse mesothelin expression correlates with prolonged patient survival in ovarian serous carcinoma. *Clin Cancer Res* **12**, 827-831 (2006).

92. Galloway, M.L., Murray, D. & Moffat, D.F. The use of the monoclonal antibody mesothelin in the diagnosis of malignant mesothelioma in pleural biopsies. *Histopathology* **48**, 767-769 (2006).

93. Cheng, W.F.*, et al.* High mesothelin correlates with chemoresistance and poor survival in epithelial ovarian carcinoma. *Br J Cancer* **100**, 1144-1153 (2009).

94. Nomura, R.*, et al.* Mesothelin expression is a prognostic factor in cholangiocellular carcinoma. *Int Surg* **98**, 164-169 (2013).

95. Thomas, A.*, et al.* High mesothelin expression in advanced lung adenocarcinoma is associated with KRAS mutations and a poor prognosis. *Oncotarget* **6**, 11694-11703 (2015).

96. Tozbikian, G.*, et al.* Mesothelin expression in triple negative breast carcinomas correlates significantly with basal-like phenotype, distant metastases and decreased survival. *PLoS One* **9**, e114900 (2014).

97. Shimizu, A.*, et al.* Coexpression of MUC16 and mesothelin is related to the invasion process in pancreatic ductal adenocarcinoma. *Cancer Sci* **103**, 739-746 (2012).

98. Rump, A.*, et al.* Binding of ovarian cancer antigen CA125/MUC16 to mesothelin mediates cell adhesion. *J Biol Chem* **279**, 9190-9198 (2004).

99. Gubbels, J.A.*, et al.* Mesothelin-MUC16 binding is a high affinity, N-glycan dependent interaction that facilitates peritoneal metastasis of ovarian tumors. *Mol Cancer* **5**, 50 (2006).

100. Uehara, N., Matsuoka, Y. & Tsubura, A. Mesothelin promotes anchorage-independent growth and prevents anoikis via extracellular signal-regulated kinase signaling pathway in human breast cancer cells. *Mol Cancer Res* **6**, 186-193 (2008).

101. Servais, E.L.*, et al.* Mesothelin overexpression promotes mesothelioma cell invasion and MMP-9 secretion in an orthotopic mouse model and in epithelioid pleural mesothelioma patients. *Clin Cancer Res* **18**, 2478-2489 (2012).

102. Bharadwaj, U., Marin-Muller, C., Li, M., Chen, C. & Yao, Q. Mesothelin confers pancreatic cancer cell resistance to TNF-alpha-induced apoptosis through Akt/PI3K/NF-kappaB activation and IL-6/Mcl-1 overexpression. *Mol Cancer* **10**, 106 (2011).

103. Bharadwaj, U., Marin-Muller, C., Li, M., Chen, C. & Yao, Q. Mesothelin overexpression promotes autocrine IL-6/sIL-6R trans-signaling to stimulate pancreatic cancer cell proliferation. *Carcinogenesis* **32**, 1013-1024 (2011).

104. Tan, K.*, et al.* Mesothelin (MSLN) promoter is hypomethylated in malignant mesothelioma, but its expression is not associated with methylation status of the promoter. *Hum Pathol* **41**, 1330-1338 (2010).

105. Hucl, T.*, et al.* High cancer-specific expression of mesothelin (MSLN) is attributable to an upstream enhancer containing a transcription enhancer factor dependent MCAT motif. *Cancer Res* **67**, 9055-9065 (2007).

106. Ren, Y.R., Patel, K., Paun, B.C. & Kern, S.E. Structural analysis of the cancer-specific promoter in mesothelin and in other genes overexpressed in cancers. *J Biol Chem* **286**, 11960-11969 (2011).

107. Marin-Muller, C.*, et al.* A tumorigenic factor interactome connected through tumor suppressor microRNA-198 in human pancreatic cancer. *Clin Cancer Res* **19**, 5901-5913 (2013).

108. Koyama, Y.*, et al.* Mesothelin/mucin 16 signaling in activated portal fibroblasts regulates cholestatic liver fibrosis. *J Clin Invest* **127**, 1254-1270 (2017).

109. Tsai, J.M.*, et al.* Surgical adhesions in mice are derived from mesothelial cells and can be targeted by antibodies against mesothelial markers. *Sci Transl Med* **10**(2018).

110. Felder, M.*, et al.* MUC16 suppresses human and murine innate immune responses. *Gynecol Oncol* **152**, 618-628 (2019).

111. Nicolaides, N.C.*, et al.* CA125 suppresses amatuximab immune-effector function and elevated serum levels are associated with reduced clinical response in first line mesothelioma patients. *Cancer Biol Ther* **19**, 622-630 (2018).

112. Ness, T.L., Hogaboam, C.M., Strieter, R.M. & Kunkel, S.L. Immunomodulatory role of CXCR2 during experimental septic peritonitis. *J Immunol* **171**, 3775-3784 (2003).

113. Henderson, R.B., Hobbs, J.A., Mathies, M. & Hogg, N. Rapid recruitment of inflammatory monocytes is independent of neutrophil migration. *Blood* **102**, 328-335 (2003).

114. Paul-Clark, M.J., Van Cao, T., Moradi-Bidhendi, N., Cooper, D. & Gilroy, D.W. 15-epi-lipoxin A4-mediated induction of nitric oxide explains how aspirin inhibits acute inflammation. *J Exp Med* **200**, 69-78 (2004).

115. Doherty, N.S.*, et al.* Intraperitoneal injection of zymosan in mice induces pain, inflammation and the synthesis of peptidoleukotrienes and prostaglandin E2. *Prostaglandins* **30**, 769-789 (1985).

116. Brown, G.D.*, et al.* Dectin-1 is a major beta-glucan receptor on macrophages. *J Exp Med* **196**, 407-412 (2002).

117. Taylor, P.R.*, et al.* Dectin-1 is required for beta-glucan recognition and control of fungal infection. *Nat Immunol* **8**, 31-38 (2007).

118. Schwab, J.M., Chiang, N., Arita, M. & Serhan, C.N. Resolvin E1 and protectin D1 activate inflammation-resolution programmes. *Nature* **447**, 869-874 (2007).

119. Bellingan, G.J., Caldwell, H., Howie, S.E., Dransfield, I. & Haslett, C. In vivo fate of the inflammatory macrophage during the resolution of inflammation: inflammatory macrophages do not die locally, but emigrate to the draining lymph nodes. *J Immunol* **157**, 2577-2585 (1996).

120. Mizoguchi, A. Animal models of inflammatory bowel disease. *Prog Mol Biol Transl Sci* **105**, 263-320 (2012).

121. Okayasu, I.*, et al.* A novel method in the induction of reliable experimental acute and chronic ulcerative colitis in mice. *Gastroenterology* **98**, 694-702 (1990).

122. Neurath, M., Fuss, I. & Strober, W. TNBS-colitis. *Int Rev Immunol* **19**, 51-62 (2000).

123. Ostanin, D.V.*, et al.* T cell transfer model of chronic colitis: concepts, considerations, and tricks of the trade. *Am J Physiol Gastrointest Liver Physiol* **296**, G135-146 (2009).

124. Seno, H.*, et al.* Efficient colonic mucosal wound repair requires Trem2 signaling. *Proc Natl Acad Sci U S A* **106**, 256-261 (2009).

125. Davies, L.C., Jenkins, S.J., Allen, J.E. & Taylor, P.R. Tissue-resident macrophages. *Nat Immunol* **14**, 986-995 (2013).

126. Hume, D.A., Robinson, A.P., MacPherson, G.G. & Gordon, S. The mononuclear phagocyte system of the mouse defined by immunohistochemical localization of antigen F4/80. Relationship between macrophages, Langerhans cells, reticular cells, and dendritic cells in lymphoid and hematopoietic organs. *J Exp Med* **158**, 1522-1536 (1983).

127. Gosselin, D.*, et al.* Environment drives selection and function of enhancers controlling tissue-specific macrophage identities. *Cell* **159**, 1327-1340 (2014).

128. Lavin, Y.*, et al.* Tissue-resident macrophage enhancer landscapes are shaped by the local microenvironment. *Cell* **159**, 1312-1326 (2014).

129. van de Laar, L.*, et al.* Yolk Sac Macrophages, Fetal Liver, and Adult Monocytes Can Colonize an Empty Niche and Develop into Functional Tissue-Resident Macrophages. *Immunity* **44**, 755-768 (2016).

130. Jenkins, S.J.*, et al.* Local macrophage proliferation, rather than recruitment from the blood, is a signature of TH2 inflammation. *Science* **332**, 1284-1288 (2011).

131. T'Jonck, W., Guilliams, M. & Bonnardel, J. Niche signals and transcription factors involved in tissue-resident macrophage development. *Cell Immunol* **330**, 43-53 (2018).

132. Wang, J. & Kubes, P. A Reservoir of Mature Cavity Macrophages that Can Rapidly Invade Visceral Organs to Affect Tissue Repair. *Cell* **165**, 668-678 (2016).

133. Minutti, C.M.*, et al.* Local amplifiers of IL-4Ralpha-mediated macrophage activation promote repair in lung and liver. *Science* **356**, 1076-1080 (2017).

134. Gautier, E.L.*, et al.* Gata6 regulates aspartoacylase expression in resident peritoneal macrophages and controls their survival. *J Exp Med* **211**, 1525-1531 (2014).

135. Rosas, M.*, et al.* The transcription factor Gata6 links tissue macrophage phenotype and proliferative renewal. *Science* **344**, 645-648 (2014).

136. Okabe, Y. & Medzhitov, R. Tissue biology perspective on macrophages. *Nat Immunol* **17**, 9-17 (2016).

137. Ruiz-Alcaraz, A.J.*, et al.* Characterization of human peritoneal monocyte/macrophage subsets in homeostasis: Phenotype, GATA6, phagocytic/oxidative activities and cytokines expression. *Sci Rep* **8**, 12794 (2018).

138. Herrick, S.E. & Mutsaers, S.E. Mesothelial progenitor cells and their potential in tissue engineering. *Int J Biochem Cell Biol* **36**, 621-642 (2004).

139. Rinkevich, Y.*, et al.* Identification and prospective isolation of a mesothelial precursor lineage giving rise to smooth muscle cells and fibroblasts for mammalian internal organs, and their vasculature. *Nat Cell Biol* **14**, 1251-1260 (2012).

140. Nouwen, E.J.*, et al.* Immunohistochemical localization of placental alkaline phosphatase, carcinoembryonic antigen, and cancer antigen 125 in normal and neoplastic human lung. *Cancer Res* **46**, 866-876 (1986).

141. Cheon, D.J.*, et al.* CA125/MUC16 is dispensable for mouse development and reproduction. *PLoS One* **4**, e4675 (2009).

142. Bot, J.*, et al.* Culturing mouse peritoneal mesothelial cells. *Pathol Res Pract* **199**, 341-344 (2003).

143. Bray, N.L., Pimentel, H., Melsted, P. & Pachter, L. Near-optimal probabilistic RNA-seq quantification. *Nat Biotechnol* **34**, 525-527 (2016).

144. Lanfrancone, L.*, et al.* Human peritoneal mesothelial cells produce many cytokines (granulocyte colony-stimulating factor [CSF], granulocyte-monocyte-CSF, macrophage-CSF, interleukin-1 [IL-1], and IL-6) and are activated and stimulated to grow by IL-1. *Blood* **80**, 2835-2842 (1992).

145. Hepler, C.*, et al.* Directing visceral white adipocyte precursors to a thermogenic adipocyte fate improves insulin sensitivity in obese mice. *Elife* **6**(2017).

146. Kanamori-Katayama, M.*, et al.* LRRN4 and UPK3B are markers of primary mesothelial cells. *PLoS One* **6**, e25391 (2011).

147. Iwahori, K.*, et al.* Megakaryocyte potentiating factor as a tumor marker of malignant pleural mesothelioma: evaluation in comparison with mesothelin. *Lung Cancer* **62**, 45-54 (2008).

148. Kojima, T.*, et al.* Molecular cloning and expression of megakaryocyte potentiating factor cDNA. *J Biol Chem* **270**, 21984-21990 (1995).

149. Yamaguchi, N.*, et al.* Characterization, molecular cloning and expression of megakaryocyte potentiating factor. *Stem Cells* **14 Suppl 1**, 62-74 (1996).

150. Zhang, J.*, et al.* Megakaryocytic potentiating factor and mature mesothelin stimulate the growth of a lung cancer cell line in the peritoneal cavity of mice. *PLoS One* **9**, e104388 (2014).

151. Pastan, I. & Hassan, R. Discovery of mesothelin and exploiting it as a target for immunotherapy. *Cancer Res* **74**, 2907-2912 (2014).

152. Kaneko, O.*, et al.* A binding domain on mesothelin for CA125/MUC16. *J Biol Chem* **284**, 3739-3749 (2009).

153. O'Brien, T.J.*, et al.* The CA 125 gene: an extracellular superstructure dominated by repeat sequences. *Tumour Biol* **22**, 348-366 (2001).

154. Bain, C.C.*, et al.* Long-lived self-renewing bone marrow-derived macrophages displace embryo-derived cells to inhabit adult serous cavities. *Nat Commun* **7**, ncomms11852 (2016).

155. Moon, C.*, et al.* Vertically transmitted faecal IgA levels determine extra-chromosomal phenotypic variation. *Nature* **521**, 90-93 (2015).

156. Jarjour, N.N.*, et al.* Bhlhe40 mediates tissue-specific control of macrophage proliferation in homeostasis and type 2 immunity. *Nat Immunol* (2019).

157. Hettinger, J.*, et al.* Origin of monocytes and macrophages in a committed progenitor. *Nat Immunol* **14**, 821-830 (2013).

158. Argueso, P., Spurr-Michaud, S., Russo, C.L., Tisdale, A. & Gipson, I.K. MUC16 mucin is expressed by the human ocular surface epithelia and carries the H185 carbohydrate epitope. *Invest Ophthalmol Vis Sci* **44**, 2487-2495 (2003).

159. Gipson, I.K.*, et al.* MUC16 is lost from the uterodome (pinopode) surface of the receptive human endometrium: in vitro evidence that MUC16 is a barrier to trophoblast adherence. *Biol Reprod* **78**, 134-142 (2008).

160. Zeimet, A.G.*, et al.* Peritoneum and tissues of the female reproductive tract as physiological sources of CA-125. *Tumour Biol* **19**, 275-282 (1998).

161. Das, S. & Batra, S.K. Understanding the Unique Attributes of MUC16 (CA125): Potential Implications in Targeted Therapy. *Cancer Res* **75**, 4669-4674 (2015).

162. Allavena, P.*, et al.* Engagement of the mannose receptor by tumoral mucins activates an immune suppressive phenotype in human tumor-associated macrophages. *Clin Dev Immunol* **2010**, 547179 (2010).

163. Dangaj, D.*, et al.* Mannose receptor (MR) engagement by mesothelin GPI anchor polarizes tumor-associated macrophages and is blocked by anti-MR human recombinant antibody. *PLoS One* **6**, e28386 (2011).

164. Belisle, J.A.*, et al.* Identification of Siglec-9 as the receptor for MUC16 on human NK cells, B cells, and monocytes. *Mol Cancer* **9**, 118 (2010).

165. Gubbels, J.A.*, et al.* MUC16 provides immune protection by inhibiting synapse formation between NK and ovarian tumor cells. *Mol Cancer* **9**, 11 (2010).

166. Tyler, C.*, et al.* The mucin MUC16 (CA125) binds to NK cells and monocytes from peripheral blood of women with healthy pregnancy and preeclampsia. *Am J Reprod Immunol* **68**, 28-37 (2012).

167. McMillan, S.J.*, et al.* Siglec-E is a negative regulator of acute pulmonary neutrophil inflammation and suppresses CD11b beta2-integrin-dependent signaling. *Blood* **121**, 2084-2094 (2013).

168. Kuziel, W.A.*, et al.* Severe reduction in leukocyte adhesion and monocyte extravasation in mice deficient in CC chemokine receptor 2. *Proc Natl Acad Sci U S A* **94**, 12053-12058 (1997).

169. Topley, N., Mackenzie, R.K. & Williams, J.D. Macrophages and mesothelial cells in bacterial peritonitis. *Immunobiology* **195**, 563-573 (1996).

170. Gundra, U.M., *et al.* Alternatively activated macrophages derived from monocytes and tissue macrophages are phenotypically and functionally distinct. *Blood* **123**, e110-122 (2014).

171. Nascimento, M., *et al.* Ly6Chi monocyte recruitment is responsible for Th2 associated host-protective macrophage accumulation in liver inflammation due to schistosomiasis. *PLoS Pathog* **10**, e1004282 (2014).

172. Hoeffel, G., *et al.* C-Myb(+) erythro-myeloid progenitor-derived fetal monocytes give rise to adult tissue-resident macrophages. *Immunity* **42**, 665-678 (2015).

173. Bellingan, G.J., *et al.* Adhesion molecule-dependent mechanisms regulate the rate of macrophage clearance during the resolution of peritoneal inflammation. *J Exp Med* **196**, 1515-1521 (2002).

174. Jonjic, N., *et al.* Expression of adhesion molecules and chemotactic cytokines in cultured human mesothelial cells. *J Exp Med* **176**, 1165-1174 (1992).

175. Mutsaers, S.E., Whitaker, D. & Papadimitriou, J.M. Stimulation of mesothelial cell proliferation by exudate macrophages enhances serosal wound healing in a murine model. *Am J Pathol* **160**, 681-692 (2002).

176. Liao, C.T., *et al.* Peritoneal macrophage heterogeneity is associated with different peritoneal dialysis outcomes. *Kidney Int* **91**, 1088-1103 (2017).

177. Bostanci, O., *et al.* Preoperative serum levels of mesothelin in patients with colon cancer. *Dis Markers* **2014**, 161954 (2014).

178. Moser, A.R., *et al.* ApcMin: a mouse model for intestinal and mammary tumorigenesis. *Eur J Cancer* **31A**, 1061-1064 (1995).

179. Gregorieff, A., Liu, Y., Inanlou, M.R., Khomchuk, Y. & Wrana, J.L. Yap-dependent reprogramming of Lgr5(+) stem cells drives intestinal regeneration and cancer. *Nature* **526**, 715-718 (2015).

180. Miyoshi, H., *et al.* Prostaglandin E2 promotes intestinal repair through an adaptive cellular response of the epithelium. *EMBO J* **36**, 5-24 (2017).

181. Dvorak, H.F. Tumors: wounds that do not heal. Similarities between tumor stroma generation and wound healing. *N Engl J Med* **315**, 1650-1659 (1986).

182. Hassan, R., Bera, T. & Pastan, I. Mesothelin: a new target for immunotherapy. *Clin Cancer Res* **10**, 3937-3942 (2004).